Effectiveness of Circuit Breakers in Mitigating Parallel Arcing Faults in the Home Run

Paul W. Brazis Jr., PhD and Fan He, PhD

NOTICE

The issuance of this Report does not constitute an endorsement of any proposed amendment and in no way implies Listing, Classification, or other recognition by UL and does not authorize the use of UL Listing or Classification Marks or any other reference to Underwriters Laboratories Inc. on, or in connection with, the product.

Underwriters Laboratories Inc., its employees, and its agents shall not be responsible to anyone for the use or nonuse of the information contained in this Report, and shall not incur any obligation or liability for damages, including consequential damages, arising out of or in connection with the use of, or inability to use, the information contained in this Report.

EXECUTIVE SUMMARY

Electrical wiring in the home can get damaged during installation or afterwards, through over-stapling, crushing, bending, penetration by screws and nails, and through rodent and insect damage. Over time cabling may degrade further due to exposure to elevated temperatures or humidity, eventually leading to arcing faults and ignition of combustibles in proximity. The length of electrical wiring between the circuit breaker panel and the first receptacle is often referred to as the "home-run". To protect the wiring from damage and subsequent potential for arcing, the National Electrical Code (NEC®) requires protection of the home run wiring using conduit or armored cabling[1] if a receptacle-mounted AFCI (known as Outlet Branch Circuit Arc-Fault Circuit-Interrupter, or OBC AFCI, in the NEC) is used in a residential circuit. This requirement was put in place since such an arc protection device would not be able to provide parallel arcing fault protection for the home run, *i.e.*, de-energize the circuit, if the fault is upstream of the OBC AFCI.

In this situation, the circuit breaker is the only means for mitigating the fault, though it is intended for protecting the wiring from overheating due to an overcurrent condition and is not intended for mitigating arcing faults. Since parallel arcing faults may deliver relatively high currents, there is the possibility that it may trip the circuit breaker and de-energize the electrical circuit. However, the ability of a circuit breaker to mitigate a parallel fault condition has not yet been well characterized in the available literature. Thus, experimental data was required to determine whether a circuit breaker may mitigate a parallel arc fault, and more specifically, the conditions under which effective protection is attained.

This research work was conducted using commercially available circuit breakers from four manufacturers in the North American market. In addition, used circuit breakers that were in service for at least 20 years were also evaluated in the event that age had a significant effect on performance. In this study, several test variables were evaluated, including manufacturer, used vs. new circuit breakers, position of the circuit breaker in the panel, and the available short circuit current. A series of circuit breaker operational tests were conducted to determine the magnetic trip currents for new and used circuit breakers. The ability of a circuit breaker to trip with parallel arc faults was then evaluated using prepared carbonized arc fault samples (per UL 1699) made with NM cable. A total of 575 experiments were performed.

Analysis of the data showed that the carbonized arc data was representative of point contact arcing, and therefore results from this work are applicable to both carbonized path and point contact arcing. The analysis also showed that circuit breaker manufacturer was not a significant influence on performance, nor was breaker age or position in the panel. The circuit breaker age did have a significant effect on magnetic trip level, with "new" breakers showing a normal distribution with mean of 212A and 99% of all breakers having a magnetic trip current at or below 300A. Used circuit breakers had broader magnetic trip

[1] More specifically, protection must include the use of RMC, IMC, EMT, Type MC, or steel armored Type AC cables meeting the requirement of 2011 NEC § 250.118. (See 2011 National Electrical Code § 210.12(A), Exception 1 for more information.

current distributions. Supported by literature reports, however, this change in magnetic trip level appears to be a result of an industry-wide design change that occurred circa 1990.

It was found in this work that a conventional circuit breaker can be an effective means of mitigating parallel arcing faults in the home run if the impedance of the home run wiring is less than a critical value based on the supply voltage and the magnetic trip level of the circuit breaker, as shown in Equation 1.

$$\rho_L L < 0.4 \cdot \frac{V_{rms}}{I_{mag}} \quad (1)$$

where

ρ_L is the resistivity per unit foot of the NM cable gauge being used;
L is the length of the "home run" in feet;
V_{rms} is the supply voltage (typically 120 V_{rms}); and
I_{mag} is the magnetic trip current of the circuit breaker.

A detailed derivation of this equation is provided in this report.

Statistical analysis was conducted to calculate the line impedance from the electrical panel to the first receptacle to ensure that 99% of all circuit breakers will trip 99% of the time, as shown in Equation 2:

$$\rho_L L < 0.4 \cdot \frac{120}{299} = 161\ m\Omega \quad (2)$$

A resistance of 161 mΩ from a 14 AWG NM cable is equivalent to 50 feet (assuming a maximum operating temperature of 90℃; at 25℃ this length of cable would measure 128 mΩ for copper conductor cable).[2] If longer runs are needed for a particular application, the wire gauge can be made larger to maintain an impedance of 128 mΩ or lower (again, measured during installation at 25℃). An evaluation of the energy released during one half-cycle when the circuit breaker magnetic trip level and home run resistance are both properly matched shows that there is a 2% probability of ignition of the NM cable if arcing were to occur.

[2] The analysis shows that the maximum impedance to achieve 300A fault current is 161 mΩ. However, the impedance of the cable will change with temperature. To ensure a maximum impedance at the maximum operating temperature (typically 90C in residential installations), a room temperature value of 128 mΩ is calculated, assuming the coefficient or resistance for copper, *k*, is 234.5℃.

TABLE OF CONTENTS

BACKGROUND

Electrical fires in homes has been attributed to nearly ten percent of all fires, with more than one-third of these caused by the fixed household wiring.[3,4,5] An arc fault circuit interrupter (AFCI) is a safety device that provides protection against fire hazards due to arcing. This arcing can result from several sources, including poor or degraded electrical connections, frayed wiring, degraded or cut wiring insulation, or penetration of metallic objects through power cords. In many of these scenarios, the magnitude of the fault current or duration of the arcing event is insufficient for the panel circuit breaker or fuse to react and remove power from the circuit.

Arcing faults can be classified into two types, series faults and parallel faults. In a series fault, the arc occurs within only one conductor and is in series with the normal flow of electrical current. Series faults occur, for example, if one conductor is nicked or cut, or an interconnect is loose or corroded. Current flow through a series fault is limited by the connected load to the circuit and therefore will not be mitigated by a circuit breaker. Parallel faults can be caused by cracked wiring insulation, contaminants, rodent damage to insulation, or metallic objects cutting through line cords (such as chair legs). In this case, the arc occurs between the supply and return wires, *i.e*., between the “hot” and “neutral” or between “hot” and “ground”, and is only limited by the available current from the panel. In this scenario, there is potential for a current of several hundred amperes. However, these arcing events may have short duration or contain long pauses between individual arcs. For this reason, parallel arcs may not cause a conventional circuit breaker to react.

AFCIs can be installed in one of two places: at the electrical panel as a replacement for a conventional circuit breaker, or at the first outlet in the circuit. In the case of the panel AFCI, all wiring in the circuit is protected beyond the panel. In the event of a series or parallel fault, the AFCI is able to disconnect power for the entire circuit. This protection includes both the household wiring as well as electrical appliances connected to the circuit.

An Outlet Branch Circuit Arc-Fault Circuit-Interrupter (OBC AFCI) is an alternative to the circuit breaker AFCI. The OBC AFCI is installed as the first outlet in a branch circuit, and is intended to provide protection to downstream branch circuit wiring, cord sets, and power-supply cords against the unwanted effects of arcing. This device also provides series fault protection to upstream branch circuit wiring, since the AFCI is able to disconnect the load and therefore stop the flow of current through the series fault.[6] As illustrated in Figure 1, parallel arc fault protection is not provided for the length of branch wiring between

[3] Babrauskas, V., “How Do Electrical Wiring Faults Lead to Structure Ignitions?” pp. 39-51 in *Proc. Fire and Materials 2001 Conf.*, Interscience Communications Ltd., London (2001).
[4] L.E. Smith and D. McCoskrie, “What Causes Wiring Fires in Residences?” pp. 19-69 *Fire Journal*, January/February (1990).
[5] “Topical Fire Report Series: Residential Electrical Building Fires,” FEMA, US Department of Homeland Security, vol. 8 iss. 2, (2008).
[6] UL Subject 1699A, Outline of Investigation for Outlet Branch Circuit Arc-Fault Circuit Interrupters, issued March 17, 2010.

the branch circuit overcurrent protection in the electric panel and the first outlet. This length of wiring is referred to as the "home run".

A 1993 UL Fact-Finding Investigation sponsored by the Electronic Industries Association (EIA)[7] recommended that the magnetic trip level of circuit breakers should be lowered to improve the ability of a circuit breaker to react to arcing faults (particularly parallel arcing faults). This resulted in an EIA proposal for the 1996 NEC Section 210-20,[8] where breakers in living and sleeping areas would be required to possess lower magnetic trip characteristics and be labeled as such. This proposal was rejected, in part citing a potential for increased nuisance tripping due to large current transients common with incandescent bulbs, compressor motors, etc.

Published literature from the early 1990s demonstrated the issue with high magnetic trip breakers failing to mitigate arcing faults: for example, as cited by Franklin.[9] Franklin's work showed that 15A breakers manufactured in North America at the time exhibited widely varying magnetic trip levels, as low as 120A and potentially exceeding 800A. He contrasted this to European 15A breakers, which magnetically tripped at 100A, allowing far less arc energy to dissipate. Franklin claims that experimental work with arcing faults shows that arcing currents are "almost always" in the range of 150A to 400A. He further states that an arcing current below 100A has "never" been observed. No substantiating information or references were supplied, or any physical information on test conditions.

The 2008 edition of the National Electrical Code permits the installation of an OBC AFCI at the first outlet to mitigate the effects of parallel arc faults occurring in the remaining portion of the branch circuit, provided that the portion of the branch circuit between the branch-circuit overcurrent device and the first outlet is enclosed in rigid metallic conduit (RMC), intermediate metallic conduit (IMC), electrical metallic tubing (EMT) or steel armored type AC cable.[10]

In December 2009 the NFPA National Electrical Code panel meetings were held to discuss comments received on proposals for revision to the 2011 NEC. Code Making Panel 2 decided to "HOLD" the AFCI Receptacle Consortium's proposal/comment to allow Outlet Branch Circuit (OBC) AFCI receptacles to be used at the first outlet in a branch circuit without requiring the fixed building wiring from the electric panel to the first receptacle to be enclosed with a steel wiring method. The substantiation provided with the

[7] "An Evaluation of Branch-Circuit Circuit-Breaker Instantaneous Trip Levels." Underwriters Laboratories Inc. For the Electronic Industries Association (EIA). 1993. R. Wagner. 92ME51901 / E87837.
[8] EIA proposal for the 1996 NEC to require "low magnetic trip" circuit breakers as a means of reducing fires due to arcing faults occurring in damaged cords to entertainment equipment such as TVs. UL conducted a Fact-Finding investigation and released its report (Ref. 7). Proposal was the following: "Section 210-20(b) Circuit breakers in Dwelling Units (New) -- Circuit Breakers for 15 A and 20 A branch circuits supplying receptacles in living and sleeping areas of dwelling units shall be a listed type identified as having specified instantaneous trip characteristics to mitigate the effects of arcing faults." "Section 240-XX(83) Circuit breakers in Dwelling Units. (New) -- Circuit breakers for 15 A and 20 A branch circuits supplying receptacles in living and sleeping areas, in accordance with Section 210-20(b), shall be listed and shall be marked "LIT" (Low Instantaneous Trip)."
[9] F. Franklin, "Circuit Breakers: The Myth of Safety," *Professional Safety*, June 1990.
[10] NFPA 70™, National Electrical Code, 2008 Edition. Article 210.12 (B), Exception 1.

public comment suggested that a conventional circuit breaker may provide some degree of parallel arc fault protection for the “home run” dependent on the available fault current, the length of the home run and the instantaneous (magnetic) trip calibration of the circuit breaker.

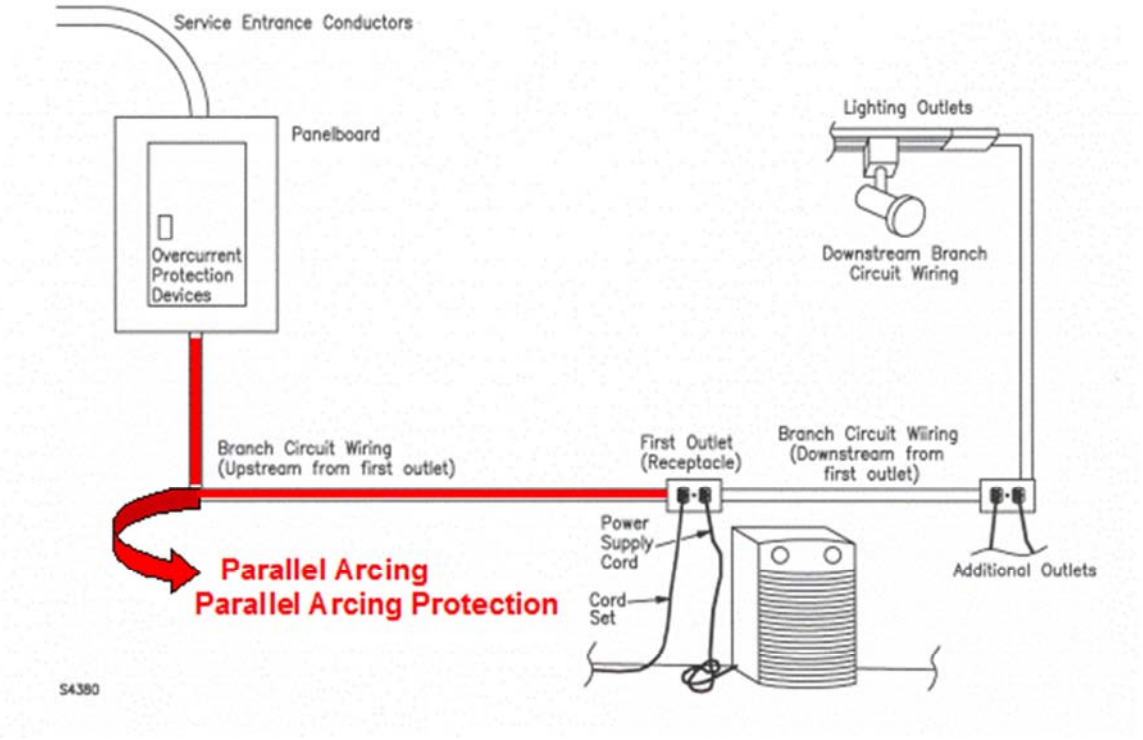

Figure 1. Parallel arcing in the “home run,” which is the length of cable between the electric panel and the first receptacle.

Parallel arcing in a circuit can occur either through development of a carbonized path or by a point contact, *e.g.*, nail penetration, that connects the hot and ground/neutral conductors. Earlier research[11] has shown that the arcing characteristics between the two only show a statistical difference with respect to the distribution of the arc strike voltage.

There is a need for data on the performance of conventional circuit breakers with respect to parallel arc faults to assist the NEC and other stakeholders in developing an informed decision.

[11] P.W. Brazis, *et al.*, “Synthetic Arc Generator for UL1699, Phase 2: Statistical Characterization of Arc Fault Behavior,” *UL Internal Report*, 2009.

Objectives

- Develop data on the performance of conventional circuit breakers with respect to parallel arc faults; and
- Identify conditions under which the circuit breakers may effectively react to parallel arc faults to prevent ignition of the NM cable.

Technical Plan

A technical plan was developed to meet the objectives as follows:

Task 1 – Characterization of circuit breaker trip performance
Task 2 – Parallel arc fault tests
Task 3 – Analysis of ignition hazard
Task 4 – Summary of findings
Task 5 – Technical report

The technical report is presented herein.

TECHNICAL REPORT

Terminology

The terminology used in the report is presented to facilitate clarity.

- **Half-cycle.** In this work, it is equivalent to 8.33 ms, or 1/120 seconds. It is defined as the time between subsequent zero-crossings of the voltage waveform (which has a fundamental frequency of 60 Hz). Each half-cycle is subdivided into 180 degrees of phase angle, corresponding to the arcsine of the voltage waveform, related to the time-varying voltage:

$$v(\theta) = V_{rms}\sqrt{2} \cdot \sin(\theta) \tag{3}$$

  For this work, phase angles of $180^o < \theta < 360^o$ has been reverted to $0^o < \theta < 180^o$, since the arcing behavior has been found by experience to be identical regardless of sign. Therefore, the absolute value of current and voltage was used for all analysis. In this work, half-cycles are the basic time unit, and are referenced as integer values corresponding to the number of half-cycles past time zero (the time when measurement was initialized).
- **Iteration number.** This is an integer value corresponding to the order in which the measurement was made for a given identical set of test parameters. For example, the first sample measured is identified as test number 1, the second is numbered 2, etc.
- **Manufacturer.** This identifies the manufacturer of the circuit breakers and panels used for each test. Four manufacturers were selected, each are identified by a letter: A, B, C, or D.
- **Age.** This denotes whether the circuit breaker is newly manufactured and not previously placed into service (“New”), or whether the circuit breaker was recovered from use in the field (“Old”).
- **Breaker Number.** This is the position where the circuit breaker was located in each panel. For each test, a different box was used per manufacturer. Identical breakers were used, with locations within the circuit breaker panel box denoted by the circuit breaker number.
- **Short-Circuit Current (A).** Also denoted as I_{max}, this is the maximum available current during a given test (limited by the resistive load added to the test circuit). The value is specified in UL 1699 with a standard method for reducing the available current for a given test (either by use of a calibrated resistive load (“Type 1”) or through the use of long lengths of coiled NM-B cable (“Type 2”)), Figure 2. For this project, only “Type 2” arrangements were used, simulating a parallel arcing fault. If the hot conductor were shorted to neutral at the location of the sample, the amount of current flowing through the circuit would be equal to I_{max}.

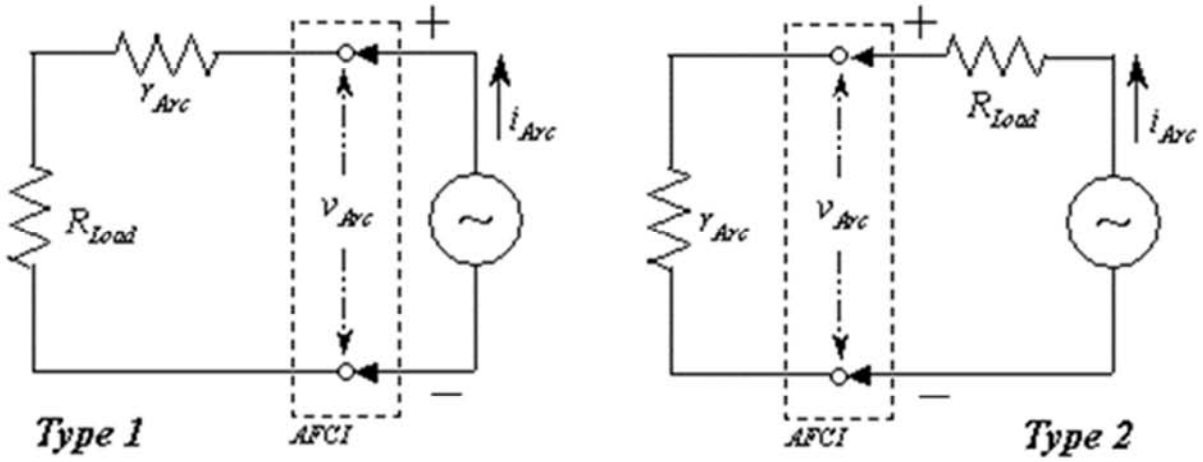

Figure 2. Two configurations of loads used in UL 1699, Section 40 tests. *(Left)* "Type 1", used in Sections 40.2 and 40.4 for low-current testing. *(Right)* "Type 2", used in Sections 40.3 and 40.5 for high-current testing.

Due to the large amount of data in each measurement (5 million data points in each of two waveforms for current and voltage), and the large number of iterations (more than 500) a convenient method of extracting a single numerical value per arcing half-cycle was required to allow for a reasonable analysis. This was achieved by the definition of several parameters for each arcing half-cycle which could be expressed as a single numerical value. For each arcing half-cycle, each of the following parameters were collected to characterize the arc (Figure 3):

- **Peak Current.** This is the maximum value (in magnitude) of the current waveform measured through the entire half-cycle.
- **Arc Strike Angle.** This is the phase value (in degrees) when the arc begins, typically characterized by a large change in current with respect to time (large *di*/*dt*). Detection was automated by finding the maximum value in the digitally filtered current waveform (Butterworth three-pole bandpass with $f_{3dB,min}$ = 10 kHz and $f_{3dB,max}$ = 100 kHz). The search was limited from zero phase angle to the phase angle corresponding to the peak current value. This technique leverages the large high-frequency component from the discontinuous change in current at the start of arcing.
- **Arc Stop Angle.** This is the phase value (in degrees) where the arc ends, characterized by a discontinuous drop towards zero current. Detection is similar to that used for identifying the arc strike angle, except search is between the phase angle of the peak current and 180 degrees. As with the strike angle, the detection software leverages the discontinuous change in current which manifests itself as a large spike in the digitally filtered current signal.
- **Arc Strike Voltage.** This is the magnitude of the voltage waveform at the moment of arc strike. This is found by first finding the arc strike angle, then finding the corresponding voltage at the same moment in time.

- **Arc Stop Voltage.** This is the magnitude of the voltage waveform at the moment of arc stop. This is found by first finding the arc stop angle, then finding the corresponding voltage at the same moment in time.

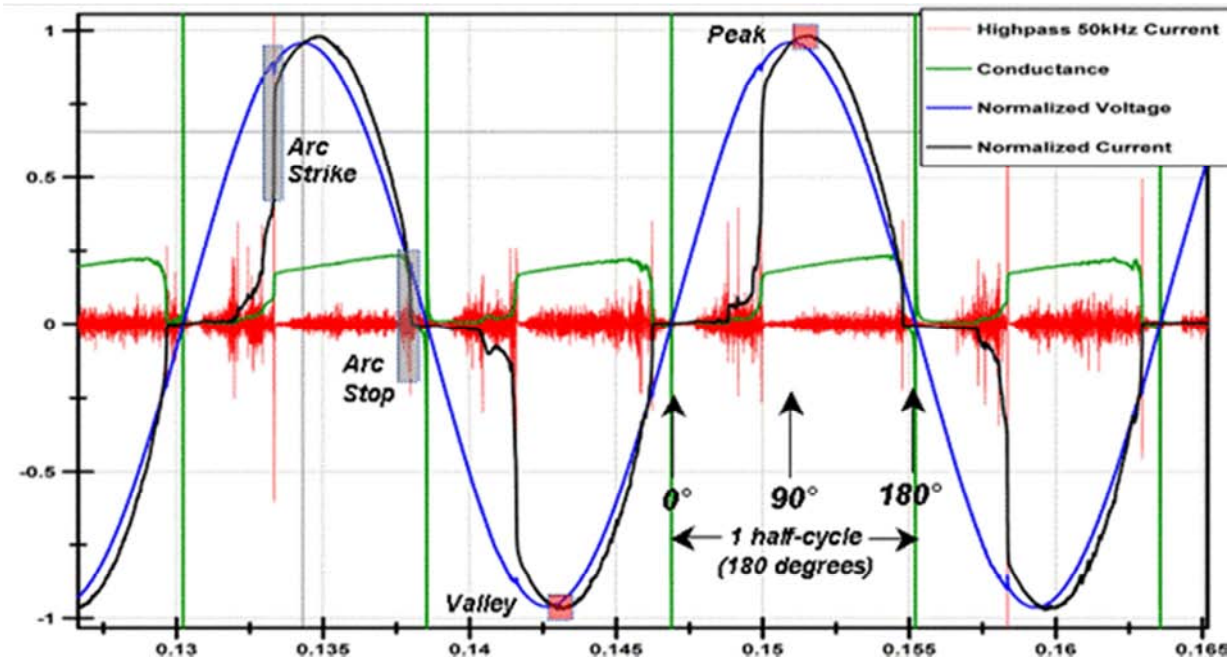

Figure 3. Current and voltage arcing waveforms, showing each arcing half-cycle.

Defining Arcing and Shorting Phenomenon

The peak current is defined in this study as the largest magnitude of current measured within each half-cycle of the waveform. These points were collected automatically using LabVIEW-based software and tabulated with corresponding variables, such as the half-cycle number, breaker manufacturer, age of circuit breaker, etc. To allow for a useful comparison of data from all tests, a normalized peak current was defined and calculated as:

$$\bar{I}_{peak} \equiv \frac{|I_{peak}|}{|I_{\max}|} = \frac{\sqrt{2}}{2} \cdot \frac{|I_{peak}|}{|I_{\max(rms)}|} \tag{4}$$

Three states of behavior were observed for peak current values: arcing behavior, non-arcing behavior, and shorted. Each of these three modes of behavior was segregated by defining two current thresholds relative to the short-circuit current I_{max} (Figure 4). A threshold of 20% I_{max} was defined as the minimum for

arcing behavior. Selection of this value can be considered somewhat arbitrary, and does not follow what is defined in UL 1699 for minimum arcing (which is defined as 5% of I_{max} in the standard). However, a very low value for the threshold, such as 5%, often would be within the large number of insignificant events (very short-duration arcing, noise, etc.) and were not likely to contribute to the understanding of the arcing behavior. At 20% I_{max} a very small percentage of data points were typically found and was a convenient threshold for defining a threshold for arcing. As this was within a "long tail" of the probability distribution function, moving this threshold ±10% in either direction would have a negligible effect on the total number of points included and therefore not affect the analysis.

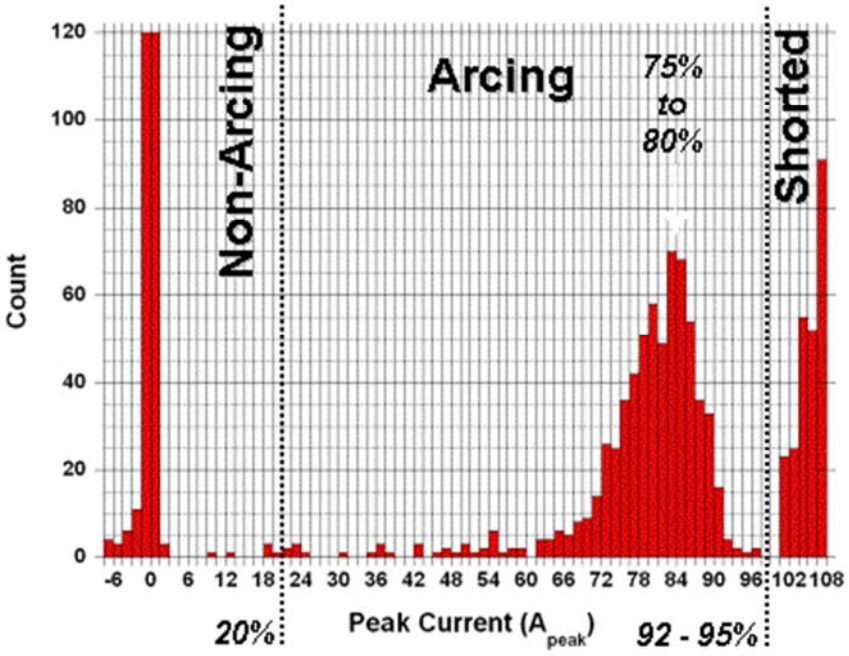

Figure 4. Representative probability distribution function for all peak current values from one series of tests, showing three modes of behavior: non-arcing (<20% I_{peak}), arcing (20% < I_{peak} < 92%-95%), and shorting (>92% to 95% I_{peak}). From Ref. 11.

Test Samples

Circuit Breakers

Four models of conventional circuit breakers available commercially in the USA were selected for this investigation. These are identified in this report as A, B, C, and D. The circuit breakers were all rated for 15A circuit current.

NM Cable

Commercially available NM cable was purchased for use in the parallel arcing tests. The NM had 14 AWG copper conductors (neutral, hot, and ground), and had a temperature rating of 90°C. The neutral and ground conductors were connected together, allowing parallel faults to occur between either hot and ground or hot and neutral. In nearly all cases, the arcing fault occurred between the hot and ground conductors.

Task 1 - Characterization of Circuit Breaker Trip Performance

The circuit breakers were characterized to determine the current levels at which magnetic tripping occurs, as well as the thermal trip time down to 75A. Each circuit breaker was subjected to symmetric short circuit fault currents until the circuit breaker cleared the fault in one half-cycle (which is defined as the instantaneous magnetic trip) to determine the instantaneous trip current. Eight circuit breakers of one model were assembled in a commercial electric panel for the characterization tests; and the tests were repeated for each of these eight breakers.

Test Procedure

A schematic of the test circuit used to develop the trip performance characteristics is shown in Figure 5. The test circuit is controlled using a closing phase angle switch. With this device, a controlled closing on the voltage waveform can be achieved. The use of controlled phase angle closing ensures that the applied voltage waveform always starts at zero degrees (at 0V immediately before the waveform swings towards positive values), so that each breaker sees the same waveform and that the number of half-cycles can be more accurately counted.

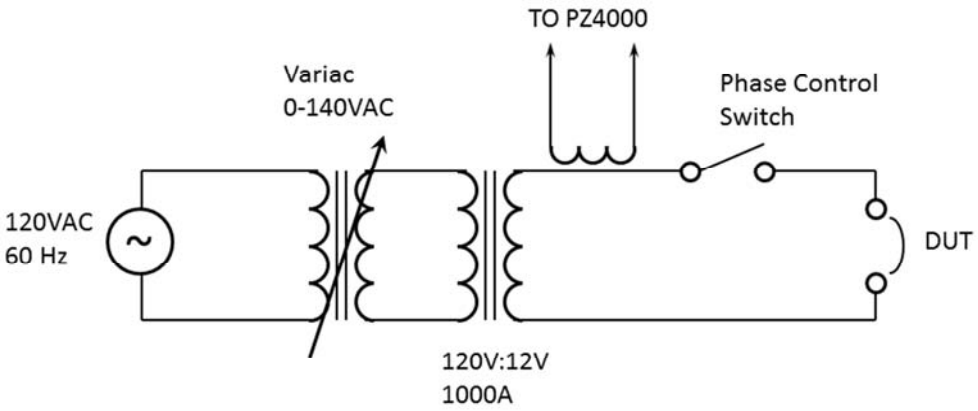

Figure 5. Circuit breaker instantaneous trip calibration test circuit

This switch and the circuit breaker under test were placed in series across a large buck-boost transformer (here, a 10:1 transformer with a secondary rated for 1000A). Control of the current was obtained through adjusting the voltage applied at the primary through a variable auto-transformer. The short-circuit current therefore was governed by changing the voltage across the internal impedance of the circuit breaker. The magnitude of the short-circuit current and the count of half-cycles were monitored through an instrument-grade current transformer connected to a Yokogawa Model PZ4000 digitizer.

Each breaker was tested at 75A, 100A, 150A, 200A, 300A, and 400A to evaluate the general response of the circuit breaker and to identify a general magnitude of the magnetic trip level. Additional tests were then conducted until the magnetic trip level was identified to the nearest 10A. The trip level was found when the minimum current required to trip the circuit breaker in one half-cycle was identified. A minimum of 2 minutes was allowed between successive trips to allow for cooling of the circuit breaker bimetal in the event that the previously applied fault current caused the circuit breaker to trip thermally.

Results

The measured magnetic trip level for each circuit breaker is shown in Table 1. Results are listed according to panel location.

Table 1. Average magnetic trip level in Amperes.

	Circuit Breaker Position in the Electric Panel							
Manufacturer	1	2	3	4	5	6	7	8
A	260	220	250	220	190	220	190	220
B	210	210	210	240	200	200	200	210
C	250	250	290	240	210	210	290	210
D	180	180	190	190	160	160	160	180

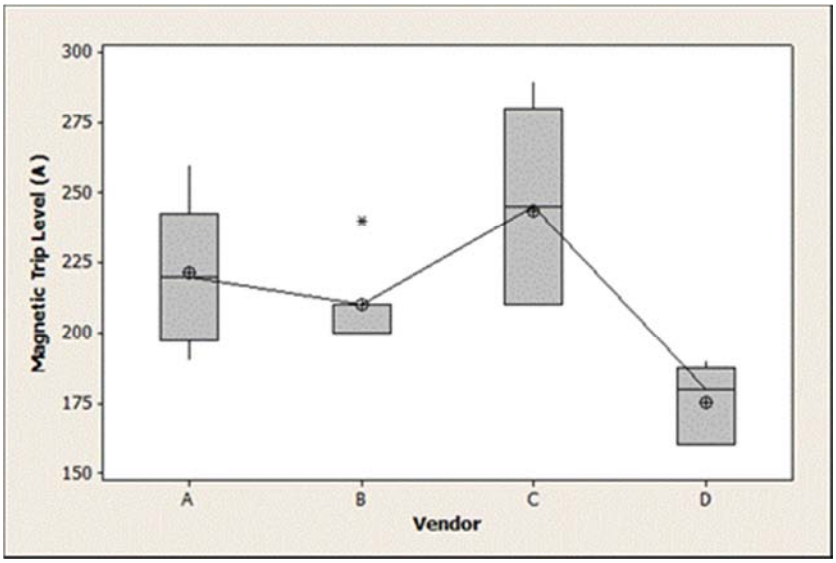

Figure 6. Boxplot showing relationship of manufacturer to magnetic trip current. The shaded box contains the middle two quartiles of the data set, the horizontal line in the middle of the shaded box is the median value, the crosshair denotes the average value, and the vertical lines show the 95% confidence interval. Asterisks denote statistical outliers.

Analysis of Circuit Breaker Characteristics

The relative influence of each variable on the normalized current was analyzed using ANOVA, and evaluated according to the resulting adjusted *R* squared ($R_{sq}(adj)$) values.[12] The influence of each test variable on the magnetic trip level (in terms of the $R_{sq}(adj)$ values) is shown in Table 2. The $R_{sq}(adj)$ values give a quantitative view of how much a particular variable influences the data. For example, the $R_{sq}(adj)$ value characterizing the influence of the manufacturer (manufacturer) of each breaker on the measured magnetic trip level is 10%, meaning that approximately 10% of the variation in the magnetic trip data can be explained by using different brands of circuit breakers. Looking at the boxplot in Figure 6, it can be seen that breakers from Manufacturer D exhibit slightly lower magnetic trip levels compared to the other three manufacturers. The $R_{sq}(adj)$ value of 10% reflects his small change in magnetic trip level. Turning now to the beaker number, which identifies the position the circuit breaker was located in the panel, the $R_{sq}(adj)$ value is 0%, which means that the breaker position had no statistical influence on the magnetic trip level. This suggests that circuit breaker position in the panel can be ignored during any further analysis of the magnetic trip level. Reviewing the histogram of the magnetic trip level for each

[12] R_{sq} is the coefficient of determination, which measures the proportion of variation that is explained by the model. For example, if R_{sq} is equal to 100%, the variable explains 100% of the behavior. Conversely, an R_{sq} value of zero would indicate that the variable has no influence. $R_{sq}(adj)$ is a modified measure of R_{sq}, which takes into account the number of terms in the model and the number of data points. A more complete explanation of *R* values can be obtained in most works on Six Sigma or other statistical sources. For example, D. Picard (ed.), *The Black Belt Memory Jogger,* Six Sigma Academy, Salem, NH: GOAL/QPC, 2002, p. 173.

breaker (Figure 7) show that the magnetic trip level for the circuit breakers is distributed normally around 213 A.

Table 2. Goodness-of-fit (*R* squared values from ANOVA) for identified independent variables influencing the magnetic trip level for each characterized breaker current level. *N* is number of data points used in each calculation of the *R* values. *P*-values are also given for each variable.

Variable	R-Sq (%)	R-Sq (adj) (%)	P	N
Manufacturer	17.05	10.14	0.078	40
Breaker Number	10.11	0.00	0.817	40

In addition to new circuit breakers, eight circuit breakers removed from residences exceeding 30 years old were characterized as well, two from each of four manufacturers were characterized. The old breaker magnetic trip levels are much more widely distributed than the data from the new breakers. Since the specific age, conditions, and other service information were not available for these circuit breakers, these "old" circuit breakers are not included here in the analysis. However, the cursory analysis of the "old" circuit breakers suggest that the magnetic trip level varies widely relative to the "new" circuit breakers and would not be expected to exhibit a readily definable distribution similar to what is shown in Figure 7. This wide distribution for circuit breakers manufactured before the year 1990 has been reported in the literature by Franklin.[9]

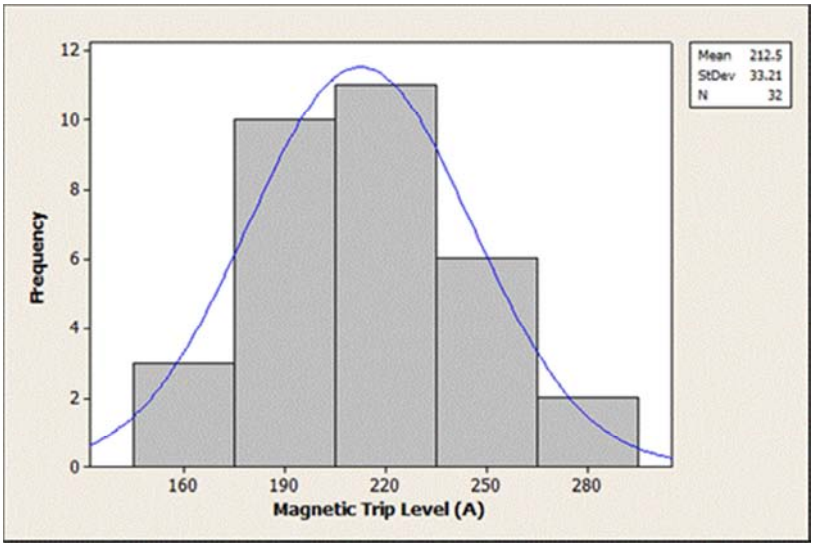

Figure 7. Histogram of the magnetic trip level for all "new" breakers.

As circuit breaker trip time is known to vary relative to the magnetic trip current, a “normalized” current magnitude is therefore defined as:

$$\bar{I}_{test} \equiv \frac{\left|I_{test(rms)}\right|}{\left|I_{mag(rms)}\right|} \tag{5}$$

Defining this normalized current allows circuit breakers possessing different magnetic trip levels to be compared together, by referencing each breaker’s performance to its magnetic trip level. The circuit breaker characterization results using this normalized current is shown in Figure 8. Representative data from tests using the “old” breakers are included here to show that newer breakers exhibit more uniform trip time behavior than the old breakers. As was mentioned previously, this old breaker data was not used for further analysis.

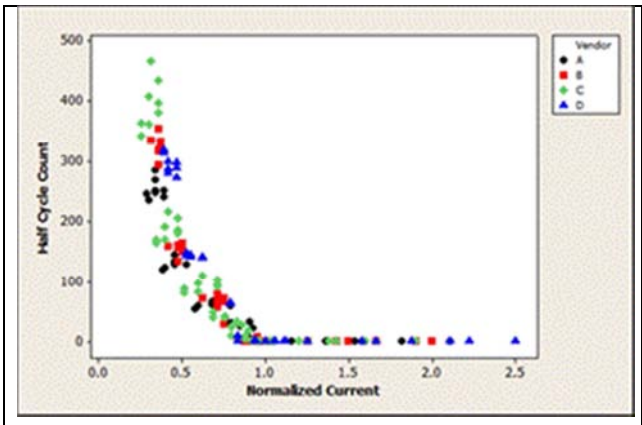

Breaker trip data for new breakers.

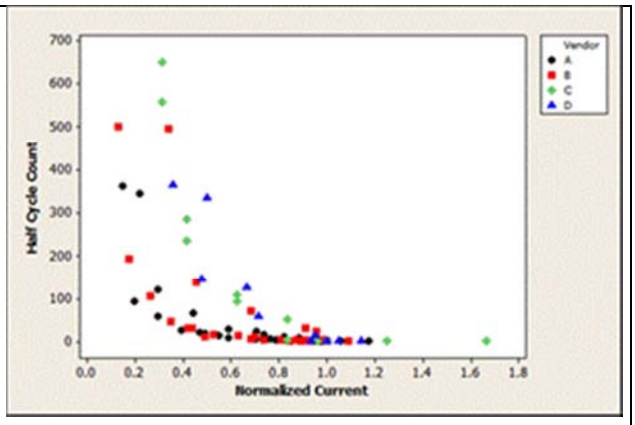

Breaker trip data for old breakers removed from service.

Figure 8. Circuit Breaker trip time shown normalized with respect to the magnetic trip level for each breaker.

The following conclusions can be deduced from the breaker magnetic trip data:

- There appears to be significant evidence in the literature that the magnetic trip level changed significantly around the year 1990. Limited experimental work with old circuit breakers confirmed this. However, insufficient information on the old circuit breakers was available to allow more in-depth analyses. Therefore, results in this work will be considered applicable only to breakers manufactured after the 1990s.
- New circuit breakers show magnetic trip levels that are normally distributed around an average value of 213 A, and a standard deviation of 33 A. This suggests that 95% of all 15 A residential

breakers will instantaneously trip at or above 277 A, and 99% of all breakers will magnetically trip at or above 300 A.

- Manufacturer (manufacturer) of the breaker did not have a major influence on magnetic trip level. Manufacturer D showed slightly lower trip levels relative to the other three brands of circuit breakers used in this study.

Task 2 - Parallel Arc Fault Tests

In this Task, circuit breakers that have been characterized in the previous Task are placed into a simulated "home run" environment that has an arcing fault present. In this Task, the resulting arcing events are analyzed statistically to determine whether characteristics of the particular circuit breaker used in the tests influence the arcing behavior. This is to explore whether any arcing characteristics (such as strike angle, peak current, etc.) are affected by design, *i.e.*, breaker manufacturer, position in the panel, etc. An ability to demonstrate statistical independence from these breaker-specific variables will allow for a simplified analysis of circuit breaker performance under more generalized arcing conditions. The following variables were identified for the parallel arcing tests:

- Available short circuit current
- Circuit breaker manufacturer
- Breaker magnetic trip level
- Position in the electric panel
- Iteration number

For each variable, at least three test iterations (replicates) were performed. A total of 575 tests were conducted in this task.

Test Procedures

Developing a Carbonized Path in NM Cable

To facilitate arcing in a consistent manner, lengths of NM cable were prepared to have a carbonized path across the conductors using the method that follows the procedure in UL 1699 - *Standard for Arc-Fault Circuit-Interrupters*,[13] Section 40.4 and briefly described herein. A transverse cut is made across the midpoint of the NM test specimen to penetrate the outer sheath and the insulations on both conductors, without damaging the copper conductor. This cut is then wrapped with two layers of electrical grade PVC tape and wrapped with two layers of fiberglass tape. A high voltage is then applied from a transformer

[13] "UL Standard for Safety for Arc-Fault Circuit-Interrupters," UL 1699, April 2006, Section 40.4, p. 40.

capable of providing 30 mA short circuit current and an open circuit voltage at least 7 kV. After approximately 10 seconds, the cable specimen is disconnected and then connected to a second transformer capable of providing 300 mA short circuit current at a voltage of at least 2 kV. After one minute of energization, the cable specimen is removed and placed in the test circuit as shown in Figure 9. The carbonized path is considered complete if a 100 W incandescent lamp in series with the path draws 0.3 A, or can start to glow at 120 V. This method is intended for SPT-2 appliance cable but has been found to provide consistent carbonized path for NM cables also.[11]

Test Arrangement

The test arrangement included a residential circuit breaker (with a known magnetic trip level) mounted in a commercially available panel manufactured by the same manufacturer as the circuit breaker (Figure 10), with the hot connection of each breaker tied to the neutral ground bar inside the circuit breaker panel (the neutral connection for the test circuit was connected directly to the arcing test sample and not through the panel). This enabled each series of circuit breakers to be tested without reconfiguring the panel, by switching the circuit breaker under test to the “on” position and leaving the other breakers in the “off” position. The available current was adjusted through the appropriate lengths of NM cable between the circuit breaker and the arcing sample to provide the necessary impedance to control the short-circuit current to the desired level, similar to that as a normal “home run”. Available current at the test bench for all tests was in excess of 1000 A. The NM cable samples were contained within a grounded metallic enclosure to reduce electrical noise from the environment and contain smoke from the test.

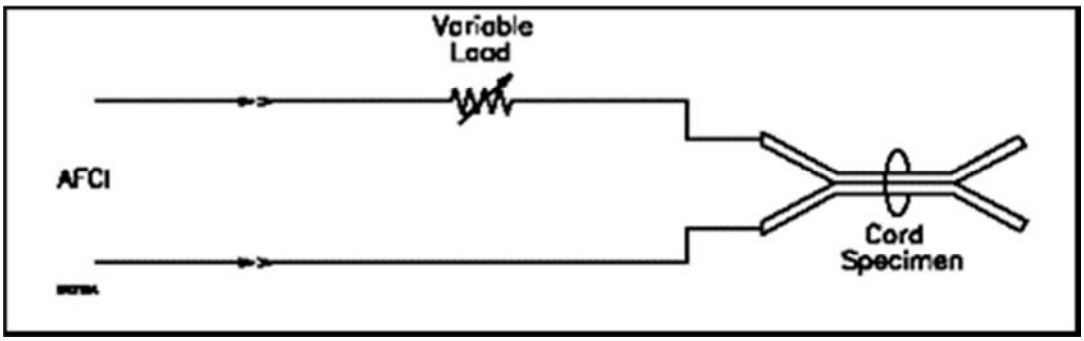

Figure 9. Electrical layout of the Arc Clearing Time Test, which was the basis of arcing tests conducted in this work. Specifically, the cord specimen was NM cable, the variable load was replaced with lengths of NM cable, and a conventional breaker was used in place of an AFCI.[13]

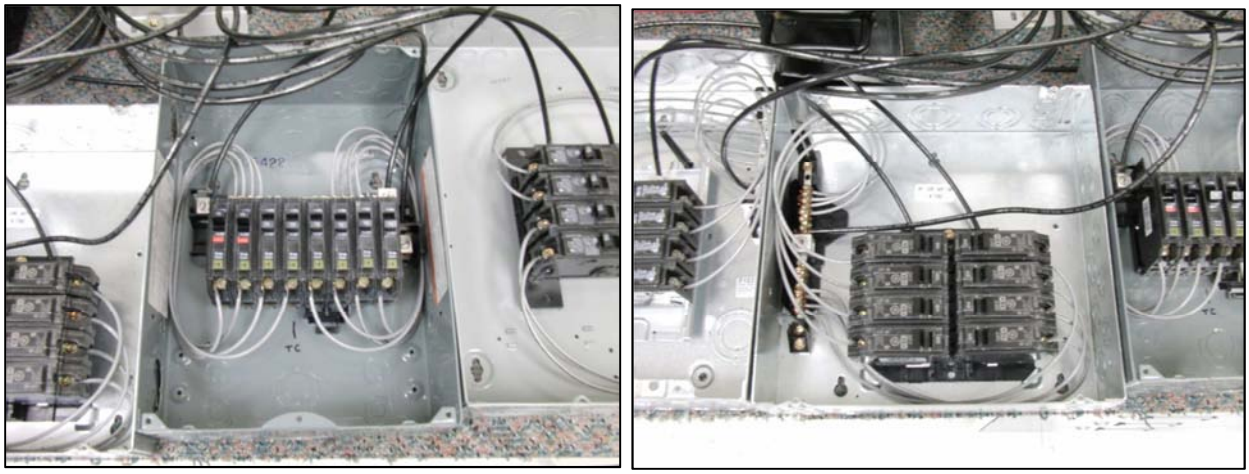

Figure 10. Representative photos of the circuit breakers under test mounted into commercially available electric panels.

Parallel Fault Arc Test Procedure

The circuit breaker under test was placed in the “on” position, and power was applied by switching the test bench circuit breaker ‘on’. The bench circuit breaker had a higher handle rating than the breakers under test (20A versus 15A for the test breakers), and was of the “high-mag” type, where the magnetic trip level of the breaker exceeds 500A. In the rare occurrence when the bench breaker tripped, the results from that iteration were not used and the test was repeated. The data acquisition was preset to acquire data when 1A current was achieved in the circuit (indicating current flow across the carbonized path). The data were then collected for 20 seconds after this trigger event. The sample rate was 250 kS/s with a sample resolution of 24 bits. An additional 200 ms of data prior to the pre-set value was also acquired. The timeframe was set to ensure that all expected arcing events were captured in their entirety during the test. In all cases, all arcing either stopped, or the circuit breaker tripped, within 10 s of the start of the test. The test data were saved in the National Instruments TDMS format for analysis.

Analysis of the Parallel Arc Fault Data

The parallel arc fault data were statistically analyzed to determine the influence of the selected variables. The test data were analyzed using automated LabVIEW software which automatically extracted parameters for each arcing and shorting half-cycle and for each test. Each NM cable sample was also visually inspected to determine whether ignition had occurred during the test. Tripping of the circuit breaker was detected though automated inspection of the voltage signal, with breaker trip detection noted when the supply voltage drops below 6 V_{rms} (5% of normal line voltage).

Details of the statistical analysis can be found in Appendix A. The results of the analysis show that arcing parameters are independent of all breaker-related test variables, and only dependent on time. Therefore, specific arcing parameters can be neglected during analysis of circuit breaker performance. Of significant importance was the demonstration that strike voltage is statistically independent of circuit breaker parameters, indicating that the results from this study are applicable to both carbonized path arcing and point contact arcing. This is because these two types of arcing were shown to be statistically different only with respect to the distribution of strike voltages. In the case of a carbonized path, the distribution of the strike voltages tends to be high (since the arc strikes only once a threshold strike voltage is exceeded), while the strike voltage of a point contact tends to be more evenly distributed between high and low voltages (since the arc strike is not dependent on a threshold voltage, with the arc striking once a point contact is made). This proof of applicability to point contact arcing is critical to this study, since attempts to reliably generate sustained and repeatable point contact arcing was not successful.

Analysis of Experimental Data on Circuit Breaker Performance

To evaluate the reaction of circuit breakers to arcing and shorting, a statistical approach was applied, investigating the likeliness of arcing to occur at a given point in time. Comparing arcing probability when a breaker is present to when it is not can be used to quantify a breaker's effectiveness in mitigating arcing faults. The probability of arcing is defined as the ratio of tests that exhibited arcing for a given point in time (characterized by the half-cycle number) to the total number of tests for the series:

$$P_{arc}(t) \equiv \frac{1}{N}\sum_{n=1}^{N} A_n(t) \tag{6}$$

where

$A_n(t)$ = 1 if arcing is present in test n at half-cycle t
$A_n(t)$ = 0 if arcing is not present
t is an integer corresponding to the half-cycle number

Whether arcing was present was determined by evaluating whether the peak current values were within 20% and 92% (or 95%) of I_{max}, as defined in the section "Defining Arcing and Shorting Phenomenon — Analysis of Normalized Peak Current".

Figure 11 *(left)* shows the probability of arcing versus half-cycle time and short-circuit current (I_{max}). Initially (during the first 100 or 150 half-cycles), the probability of arcing decreases as the half-cycle number increases. This drop in probability can be characterized by an exponential relationship:

$$P(t) = Ae^{Bt} \tag{7}$$

The plot shown in Figure 11 *(left)* is not convenient for a comparative evaluation of the rate of decay of the probability of arcing (in order to derive information such as the expected length of the arcing event, the probability of observing more than eight half-cycles to comply with UL 1699, etc.). A more convenient comparison is to use the coefficient *B*, which characterizes the rate of change of the probability of arcing in time. (The parameter *A* is always approximately 1, since all tests were triggered once arcing was initiated, meaning that at time zero the probability of an arc is equal to 1.) The trend of parameter *B* with respect to short-circuit current is shown in Figure 11 *(right)*. A more negative value for *B* means that the probability decreases more rapidly with increasing time. A zero or positive value for *B* would denote that the probability is constant or increasing with time, respectively.

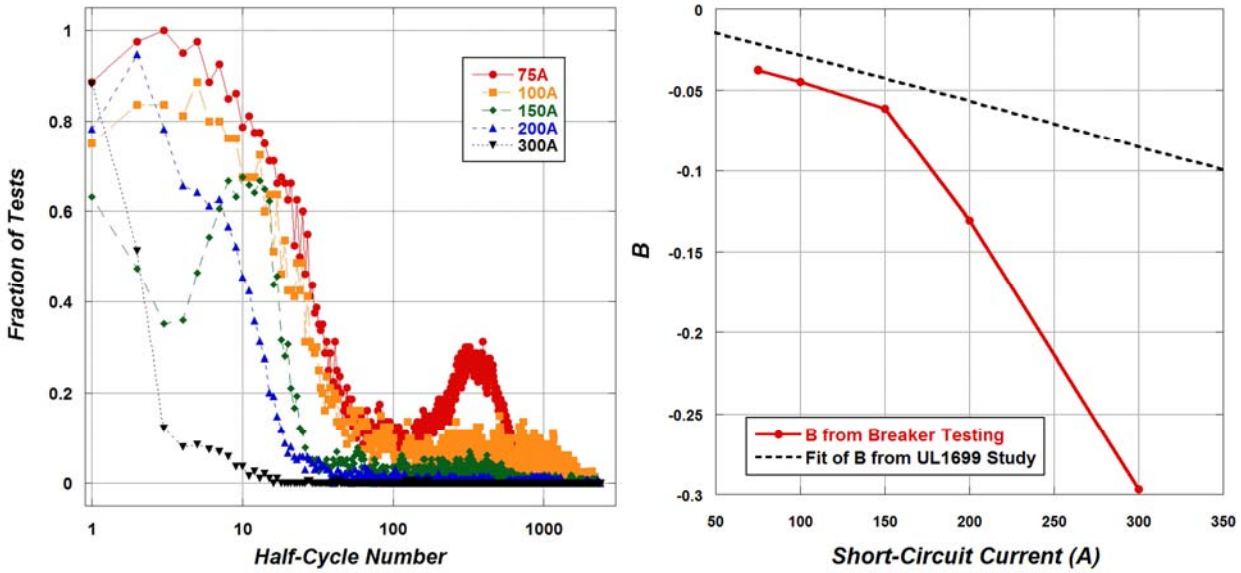

Figure 11. *(Left)* Probability of arcing versus time and short-circuit current, which shows shorter expected arcing event lengths with increasing available current. *(Right)* Parameter *B* from exponential curve fits of data in *(left)*. Dashed line is fit of series of *B* values from NM-B tests conducted in previous study (Ref. **19**). Note that the slope of the fit matches that for the circuit breaker work at lower short-circuit currents.

Parameter *B* becomes more negative as short-circuit current increases, suggesting a shorter arcing event as the current increases. In a previous study evaluating arcing behavior during UL 1699 tests (Ref. 11), the probability of arcing was similarly analyzed and the series of parameter *B* values were fit to a linear curve to derive an empirical equation relating parameter *B* to the short-circuit current I_{max}, resulting in the following (in units of Half-Cycle^{-1}):

$$B(I_{max}) = -0.000282 \cdot I_{max} - 0.00614 \tag{8}$$

This line is shown in Figure 11 *(right)* for comparison to the *B* values obtained in this work. As the parameter *B* denotes a rate of change in the probability of arcing over time, it can be considered a measure of the expected duration of an arcing event, with more negative *B* values denoting shorter expected arcing events. The results from the UL 1699 work were for characterizing the expected duration of the arcing event without any mitigation of that event. In other words, the line in Figure 11 *(right)* reflects that expected length of time an arcing event will occur on its own. Comparatively lower values for *B* for an arcing mitigation method would therefore denote that the mitigation method is shortening the expected arcing duration at a particular I_{max}. As can be seen, the *B* values are more negative for the circuit breaker work than for the unimpeded events, deviating from one another as short-circuit current increases. This reflects the increased reaction of the circuit breaker as the current increases. It is noted that this increased breaker response as current increases deviates the trend of $B(I_{max})$ away from a linear relationship. However, $B(I_{max})$ for the circuit breaker data is nearly linear at I_{max} at and below 150 A. Interestingly, the slope of $B(I_{max})$ between 75 A and 100 A is identical to that from the UL 1699 study (-0.000282 $A^{-1}\cdot$Half-$Cycle^{-1}$).

With these values for *B*, a relationship may be developed to compare mitigation techniques to unimpeded arcing duration. This relationship can then be used to calculate a timeframe when the probability of arcing falls to a particular level, *i.e.*, falls to 50% or 10% of the magnitude of the short-circuit current:

$$P(t, I_{max}) = e^{tB(I_{max})} \tag{9}$$

Using the value of *B* calculated from the parallel arcing results, the probability of unimpeded arcing is presented in Equation 10:

$$P(t, I_{max}) = e^{t(-0.000282\cdot I_{max} - 0.00614)} \tag{10}$$

The data after 100 half-cycles shows a reverse, exhibiting an increase in the probability of arcing with time. This increase peaks at approximately 300 to 400 half-cycles, then falls off again. The increase is most significant for the 75 A tests, and decreases rapidly as the short-circuit current increases. The trend does not seem to be an artifact of circuit breaker operation, and may suggest a long-timeframe oscillation in arcing behavior. The pause in arcing for 1 to 2 seconds may suggest thermal contraction during this time, leading to a re-strike of the event. These comments are purely speculative and have not been studied further here. However, since the second series of arcing occurs only after a large number of arcing half-cycles have already occurred, a probability of fire is expected to be very high and therefore any mitigation method would need to react before this second event begins.

Circuit Breaker Reaction to Shorting

Figure 12 *(left)* shows the probability of shorting with time, which was collected in a similar manner as was done for arcing. As the data show, shorting is much more prevalent at or below 150 A. Shorting tends to occur earlier as the current rises: at 75 A, peak shorting occurs after 100 half-cycles, peaking around 300 half-cycles; shorting at 150 A tends to be present only in the first 10 to 12 half-cycles of the event. Interestingly, arcing at 100 A is less prevalent and occurs with relatively equal probability during the first 100 half-cycles. These results do not show any clear trend, but do show that short-circuit current plays a significant role in influencing shorting behavior (this matches the statistical results discussed in the following section, “Analysis of Circuit Breaker Performance ”).

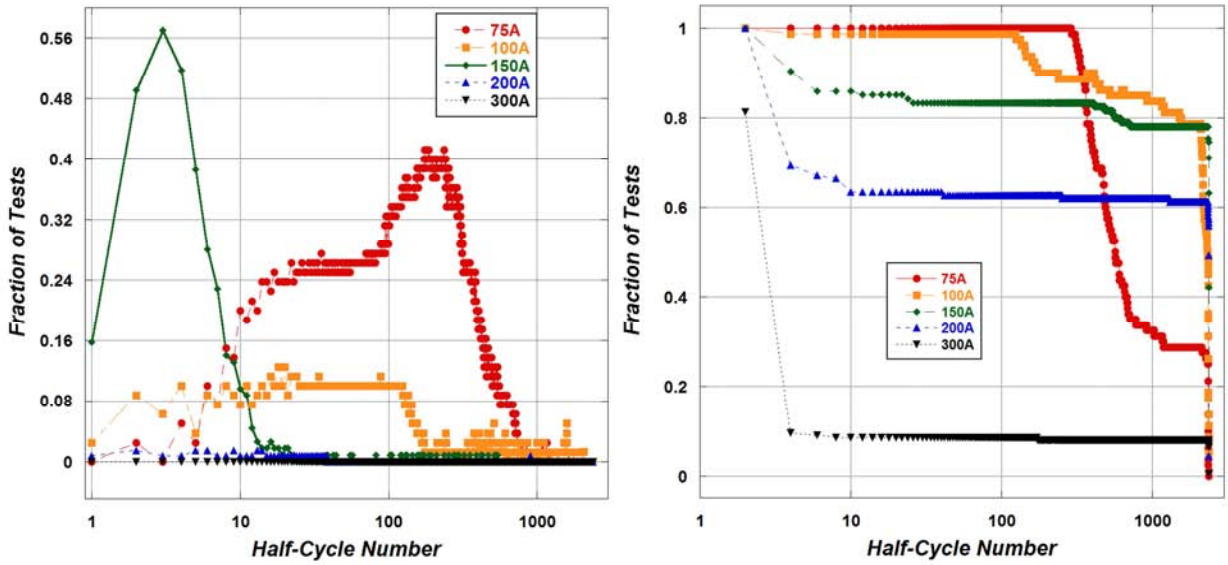

Figure 12. *(Left)* Probability of shorting versus time and short-circuit current, which shows marked shorting at 75A and 150A, and minimal shorting above 150A. Shorting also tends to occur earlier as the short-circuit current rises. *(Right)*.

Circuit Breaker Reaction to Arcing and Shorting

Figure 12 *(right)* shows the fraction of circuit breakers providing power over time. This therefore shows the fraction of circuit breakers which have not tripped at a function of time. The figure shows that, if an eight half-cycle reaction time is required of a breaker to effectively replace an AFCI in mitigating a parallel fault, significant protection is not achieved until the short-circuit current exceeds 300 A (which exceeds the magnetic trip level of most breakers in this work). At 300 A, roughly 90% of all breakers were tripping within eight half-cycles. However, at or below 100 A, virtually zero of the circuit breakers reacted within this timeframe, and continued to not react to the fault for several hundred half-cycles.

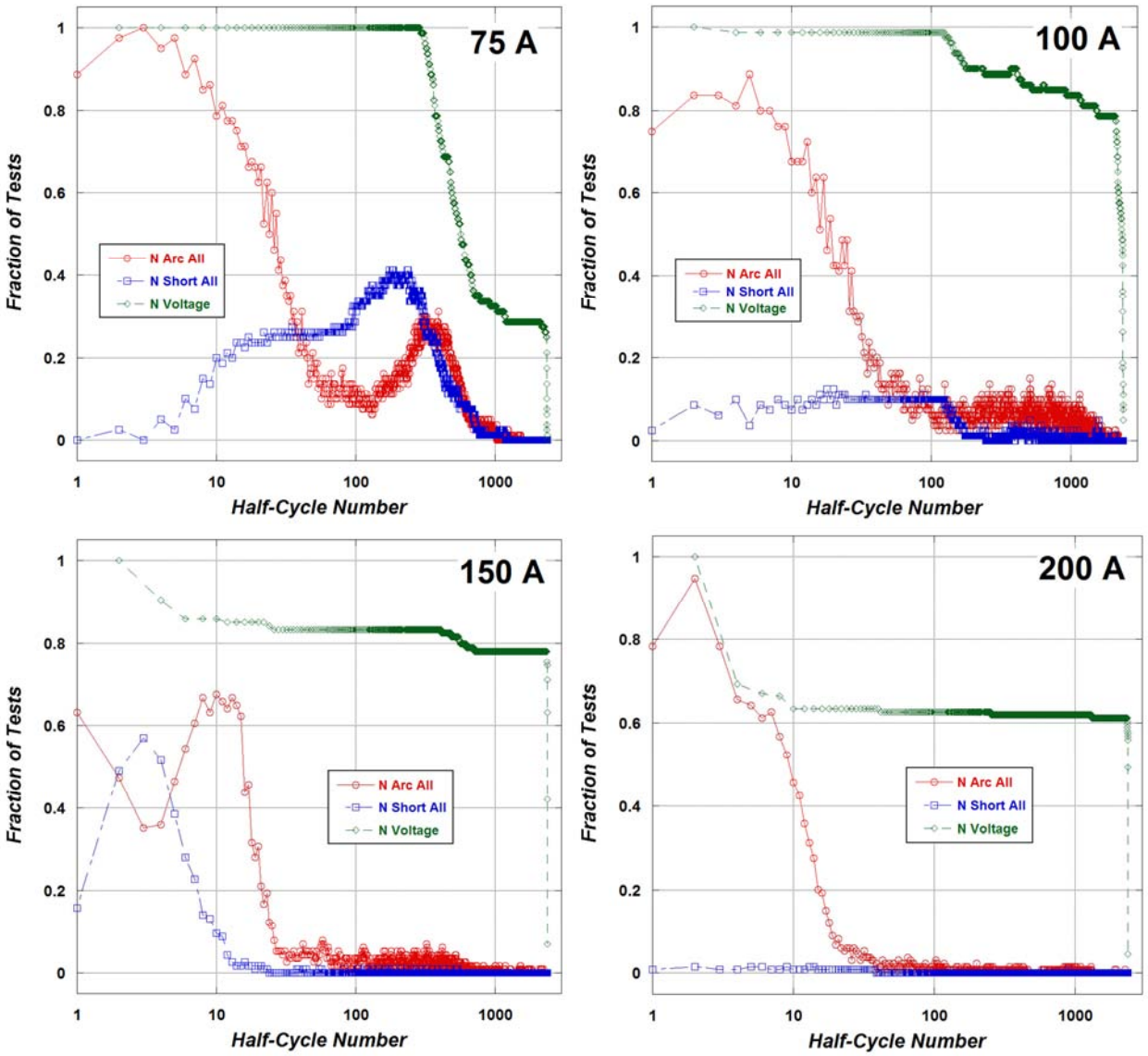

Figure 13. Voltage trip data shown with arcing and shorting probabilities for 75 A through 200 A.

A more clear analysis can be done by overlaying the arcing and shorting data on top of the voltage data. This is shown for 75 A through 200 A in Figure 13. The data at 300 A are not shown since most circuit breakers tripped very quickly, since the magnetic trip level had been exceeded. Therefore, this analysis gives a view of circuit breaker reaction to arcing and shorting faults while operating largely in the thermal trip regime. From the data, it can be seen that breakers tend to be rather insensitive to arcing faults at or below 150 A. At these short-circuit currents, breakers tended to trip once shorting has occurred (this can

be empirically viewed by comparing the change in the number of circuit breakers providing voltage to the arcing and shorting peaks). In particular, virtually all breakers continue to provide power through to peak time of arcing at 75 A and at 100 A, showing more reaction to shorting events. The exception is at 200 A, but virtually no shorting occurred at this current level.

These results are expected due to the nature of the operation of a circuit breaker, as they are by design intended to delay tripping at intermediate fault currents to prevent nuisance tripping during transient surge events, such as during startup of large motors and when lighting is turned on. Shorting tends to exhibit higher peak currents relative to arcing (roughly 20% higher), so shorting events are expected to magnetically trip a breaker at lower fault currents relative to an arc. Additionally, since a shorting fault sinks more power within a half-cycle relative to an arc fault (since shorts deliver the full fault current over the entire half cycle, where an arc fault delivers no power before a threshold strike voltage is attained), wiring temperature is expected to rise at a faster rate during a shorting event, triggering the circuit breaker bimetal more quickly.

Probability of Arcing for Eight or More Half-Cycles

Using the empirical results discussed in this section, a probability of achieving eight or more half-cycles within 0.5 seconds can be calculated to assess the ability of circuit breakers to mitigate a parallel fault based on the criteria in UL 1699. This probability then may be compared to the results obtained through unmitigated arcing conditions under the same test conditions. The difference in probabilities then characterizes the effectiveness of a breaker in providing protection when compared to the AFCI criteria in UL 1699.

The general method used here is to leverage the exponential curve fitting of the incidence of arcing with time. Here only this initial decay will be considered: this is justifiable since according to UL 1699 the AFCI must react within 0.5 s, or 60 half-cycles. As before, the values for *A* and *B* were found experimentally through least-squares curve fitting of the arcing probability data. Using this formula, numerical probabilities of eight or more half-cycles occurring within 0.5 seconds can be calculated. The derivation of such a formula resembles that for a Bernoulli distribution, since the presence of an arcing event in a given point of time can be characterized by a probability, $p(t)$, and a lack of arcing by its inverse, $1 - p(t)$. However, Bernoulli distributions assume that the probability through time is constant. In the case here, the probability of arcing with respect to time is not constant, but follows an exponential function.

The probability of exactly zero arcing events occurring in one half-second can be expressed as the following:

$$P_0 = \prod_{t=1}^{60} \left(1 - p_t\right) \tag{11}$$

where p_t is the probability of an arc at half-cycle number t. This expression is simply the product of the probability of not obtaining an arc in any of the 60 half-cycles during the 0.5 second test. The probability of obtaining exactly one arc during the test requires the summation of all combinations of one arc (the arc can appear in any one of the sixty half-cycles). This therefore can be expressed as:

$$P_1 = \sum_{n=1}^{60}\left[p_n \prod_{t=1}^{59}(1-p_t)\right] = \sum_{n=1}^{60}\left[\frac{p_n}{(1-p_n)} \prod_{t=1}^{60}(1-p_t)\right] = P_0 \sum_{n=1}^{60} \frac{p_n}{(1-p_n)} \tag{12}$$

where p_n is the probability of an arc at time n. Expanding to exactly two arcs is calculated similarly, including all combinations of the two arcs:

$$P_2 = \frac{1}{2} P_0 \sum_{m=1}^{60}\sum_{n=1}^{60} \frac{p_m p_n}{(1-p_m)(1-p_n)} - P_0 \sum_{n=1}^{60} \frac{p_n^2}{(1-p_n)^2} \tag{13}$$

The one-half term is added since each combination of m and n are summed twice (for example, m = 2, n = 3 and m = 3, n = 2 are the same combination and therefore should be counted only once). For two or more arcs, each must occur at different half-cycles; therefore, combinations where $m = n$ above need to be removed since they cannot occur. For y arcs, this formula can be generalized as:

$$P_y = \frac{1}{y!} P_0 \sum_{z=1}^{60} \cdots \sum_{m=1}^{60}\sum_{n=1}^{60} \frac{p_m p_n \cdots p_z}{(1-p_m)(1-p_n)\cdots(1-p_z)}, \text{ where } m \neq n \neq \ldots \neq z. \tag{14}$$

A more efficient version of this equation can be obtained if the ranges of the summations are bounded in the following manner, which eliminates the redundant terms:

$$P_y = P_0 \sum_{z=1}^{60-y} \cdots \sum_{l=y+k-3}^{58} \sum_{m=y+l-2}^{59} \sum_{n=y+m-1}^{60} \frac{p_m p_n \cdots p_z}{(1-p_m)(1-p_n)\cdots(1-p_z)} \tag{15}$$

This version is critical for solving for y values above 5, since the number of computations required to solve the original equation quickly become impractical. For example, y = 7 would require 60^7 or 2.8 trillion factors to be summed, each factor requiring a minimum of 59 multiplications to generate. With available computing abilities, this would take roughly 7 months to solve for a single value of P_7. In contrast, the more efficient version requires only 50 million terms and can be solved in approximately one hour (reduction in complexity is by a factor of y!. For P_7, 7! = 5040.).

To calculate the probability of seven or fewer arcs in 0.5 seconds, eight probabilities for zero to seven arcs are calculated, then summed as presented in Equation 16:

$$P_{0,7} = P_0 + \sum_{y=1}^{7} P_y \tag{16}$$

where P_y is as was expressed previously. Therefore, calculation of $P_{0,7}$ above (Table 3) gives the probability that a particular circuit breaker will be successful in mitigating the parallel arcing fault at a particular fault current, or in the unmitigated case, the probability that seven or fewer arcs will naturally occur before self-extinguishing at that short-circuit current level. As is seen, the probability of eight or more half-cycles is virtually unchanged when the short-circuit current is below 300A, showing that circuit breakers are ineffective in mitigating arcing at these current levels. At 300A, the probability of eight or more arcs changes dramatically, showing that a circuit breaker is very effective at mitigating arcing at this level. Since 99% of all breakers magnetically trip at or above 300A (as discussed previously and shown graphically in Figure 7), it is concluded that effective mitigation of arcing is only achieved when the magnetic trip level is exceeded.

Table 3. Evaluation of the effect of circuit breaker mitigation of arcing faults, based on exponential fitting of time-based arcing data. *A* and *B* are the exponential fitting parameters used for calculating probabilities. P_7 is probability of exactly seven arcs in 0.5 seconds, $P_{8,60}$ is probability of eight or more half-cycles occurring, or the probability that the test will fail UL 1699 criteria.

	Unmitigated Case				**Breaker Mitigated Case**			
Short-Circuit Current (A)	*A*	*B* (Half-Cycle^{-1})	P_7	$P_{8,60}$	*A*	*B* (Half-Cycle^{-1})	P_7	$P_{8,60}$
75	0.84008	–0.03644	1.7^{-5}	**1.0000**	1.2020	–0.037462	2.7^{-13}	**1.0000**
100	0.71862	–0.04833	8.8^{-3}	**0.9867**	1.0841	–0.044532	6.9^{-8}	**1.0000**
150	0.64930	–0.03998	5.6^{-3}	**0.9916**	0.85635	–0.061453	0.010	**0.9844**
200	0.95322	–0.07171	0.013	**0.9806**	1.3553	–0.13071	0.082	**0.8827**
300	0.92577	–0.08326	0.057	**0.9033**	0.81587	–0.29683	1.1^{-3}	**0.0001**

The fault current can be directly translated to the distance between the circuit breaker and location of the parallel fault. Ultimately, this table of probabilities could be used to quantify the risk of failing to mitigate a parallel fault based on maximum length of home run wiring. Potential code changes resulting from this investigation may include an upper bound on home run wiring impedance, *i.e.*, maximum allowable length for a given wire gauge, or minimum required magnetic trip times for circuit breakers. These parameters would be dependent on the maximum acceptable probability of a circuit breaker failing to react to an arcing fault within eight half-cycles.

Limitations with the Arc Probability Analysis

Through the design-of-experiment for this work, a goal was to include circuit breakers from most major manufacturer, as well as a wide range of magnetic trip levels that may be encountered (at least within 15 A residential circuits). The selection of circuit breakers was successful in obtaining a wide range of magnetic trip levels, from 150 A to 570 A. Both newly manufactured, as well as old breakers removed from service were also obtained to determine whether aging effects and/or changes in breaker design had a significant influence. However, though it is of the opinion of the authors that the circuit breakers used in this work are representative of what is in service in the field, it is not known whether the specific distribution of the circuit breaker performance closely matches all installations in the field. This survey was not conducted here, nor is it likely to result in beneficial data: breakers encountered in a given installation are likely to vary widely based on age, manufacturer, aging conditions, and numerous other factors. Therefore, though it is strongly believed that the empirical results from this work will give an accurate view of circuit breaker performance, it is to be remembered that specific installations may vary from this case. Therefore, these results should be considered “representative” of what is to be expected in real-world installations. These limitations, as well as a method to deal with a variable magnetic trip level, will be explored in more detail later in the following sections.

Analysis of Circuit Breaker Performance Normalized to Magnetic Trip Level

As is known from the circuit breaker calibration discussed in Task 1, the circuit breaker response time is dependent on the magnetic trip level of that particular circuit breaker. Furthermore, it was observed that two breakers despite being of the same model from the same manufacturer may exhibit different magnetic trip levels. This variability in performance was a key limitation in the prior analysis of circuit breaker performance with respect to short-circuit current. As was seen in Figure 8, when breaker performance is expressed relative to the magnetic trip level, performance for “new” breakers is very uniform, even among manufacturers. Therefore further analysis would benefit using a “normalized” current magnitude, defined as:

$$\bar{I}_{test} \equiv \frac{\left|I_{test(rms)}\right|}{\left|I_{mag(rms)}\right|} \tag{17}$$

Defining this normalized current allows breakers possessing different magnetic trip levels to be compared together. Using this normalized current and key test parameters, the correlation of each key variable can be analyzed, again using ANOVA. Appendix B contains the results of this analysis. Through a final analysis of these results, only short-circuit current shows a significant influence on the test variables, and therefore all other variables can be neglected for further study. Breaker age and breaker number showed

very low *R* value (<5%) for all variables, and therefore are not significant parameters in this work. Though manufacturer showed moderate influence on normalized current and time of circuit breaker trip, this was an artifact of the Manufacturer D breakers having consistently lower magnetic trip levels relative to the other three manufacturers. This would result in Manufacturer D breakers having an overall higher normalized current. Since the magnetic trip level is lower than other manufacturers, it would be expected that Manufacturer D breakers trip more often throughout all testing. If the current level is normalized to the magnetic trip level of each breaker, the influence of manufacturer becomes insignificant, and breaker trip time becomes decoupled from the magnetic trip level. The iteration number showed moderate correlation to all test variables; however, further investigation by short-circuit current (Figure 34) reveals that the correlation is an artifact of increased number of iterations at higher short-circuit currents. Once this is taken into consideration, the iteration number shows negligible effect on the test variables.

Circuit Breaker Performance Relative to Magnetic Trip Level

From the statistical analysis of the arcing behavior, most test variables can be eliminated from consideration, including circuit breaker position, manufacturer, age, iteration number, and absolute magnetic trip level. As the analysis shows, the short-circuit current is the dominant variable controlling circuit breaker magnetic trip level. Therefore, to be able to compare performance between circuit breakers with different magnetic trip levels, the normalized current (Equation 17) will be used as defined earlier. A normalized current of 1.0 denotes operation at the circuit breaker magnetic trip level; values less than 1 denote operation below the magnetic trip level (operating in the thermal trip regime); and values greater than 1.0 denote operation above the magnetic trip level. As it has already been discussed that specific arcing behavior is independent of the test variables (except for time), and thus only the number of arcing events and their occurrence in time are considered for the remainder of this work.

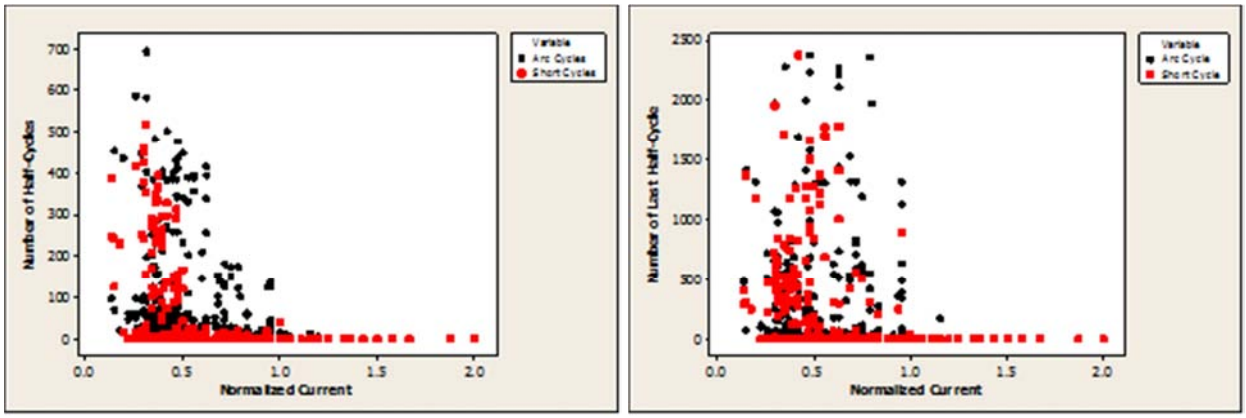

Figure 14. *(Left)* Number and *(right)* time of last arcing and shorting half-cycle.

As can be seen in each plot in Figure 14, though arcing and shorting greatly diminishes when the magnetic trip level is reached, significant arcing may occur at or below a normalized current of 1.2. Figure

14 also shows the number and time of last arcing and shorting half-cycle as a function of normalized current. As can be seen, below the magnetic trip level, both arcing and shorting can be significant and of a very long duration. It was observed that though the number of shorting half-cycles passing through the circuit breaker is greatly reduced when half the magnetic trip level is reached, significant amounts of arcing may occur above the magnetic trip level, with one test even showing 12 arc half-cycles at 1.15 times the magnetic trip level. The time of last arcing or shorting event shows greatly diminished duration of event when the magnetic trip level is reached, but nonzero events were recorded, including one occurring over a period of 171 half-cycles, again at 1.15 times magnetic trip level.

Table 4. Results from normally-distributed cumulative distribution fit from failed breaker tripping data (as shown in Figure 15, *right*).

Percent Tripped	Normalized Current	Percent Tripped	Normalized Current
1	0.126895	70	0.766266
2	0.188034	80	0.837413
3	0.226824	90	0.936081
4	0.256005	91	0.949359
5	0.279741	92	0.963784
6	0.299945	93	0.979645
7	0.317659	94	0.997360
8	0.333520	95	1.01756
9	0.347945	96	1.04130
10	0.361223	97	1.07048
20	0.459892	98	1.10927
30	0.531039	99	1.17041
40	0.591831	99.9	1.34174
50	0.648652	99.99	1.48276
60	0.705473	99.999	1.60519

Consideration only of number of arcing and shorting half-cycles does not include whether the circuit breaker reacted to the arcing, since some arcing events may have extinguished themselves without any breaker action. Figure 15 *(left)* shows the time at when the circuit breaker tripped thus removing power from the circuit. Values at 2375 half-cycles (which is the time when data gathering during the test was stopped) denote a breaker that failed to trip during the 20-second test. Values less than 2375 denote breakers that succeeded in tripping. As was expected, breakers tended to trip more quickly as the current approached the magnetic trip level. However, many instances of circuit breakers failing to trip were observed up to 1.2 times the magnetic trip level. In Figure 15 (*right*) and Table 4, the circuit breaker data which failed to trip (where last voltage cycle was 2375) is used to calculate a cumulative distribution

function to determine the probability that a breaker would trip for a given normalized short-circuit current. As can be seen in Table 4, breakers are expected to trip during an arcing event only 95% of the time when the short-circuit current is equal to the magnetic trip level (normalized current equal to 1.0). A breaker will trip 99% of the time during an arcing event only once the short-circuit current exceeds approximately 1.2 times the magnetic trip level.

To understand the reason why a short-circuit current needs to exceed the magnetic trip level to ensure tripping during arcing, the probability distribution function of the peak arcing current needs to be re-examined (Figure 4). As can be seen, peak arc current is not expected to exceed 92% of short-circuit current (I_{max}), and will have a median value of approximately 80% of I_{max}. Taking the inverse of these values, this shows that, at minimum, the short circuit current needs to be 1.08 times the magnetic trip level (since 92% of 1.08 will equal the magnetic trip level of 1.0), and will not achieve the median value until 1.25 times the magnetic trip level (80% of 1.25 equals 1.0).

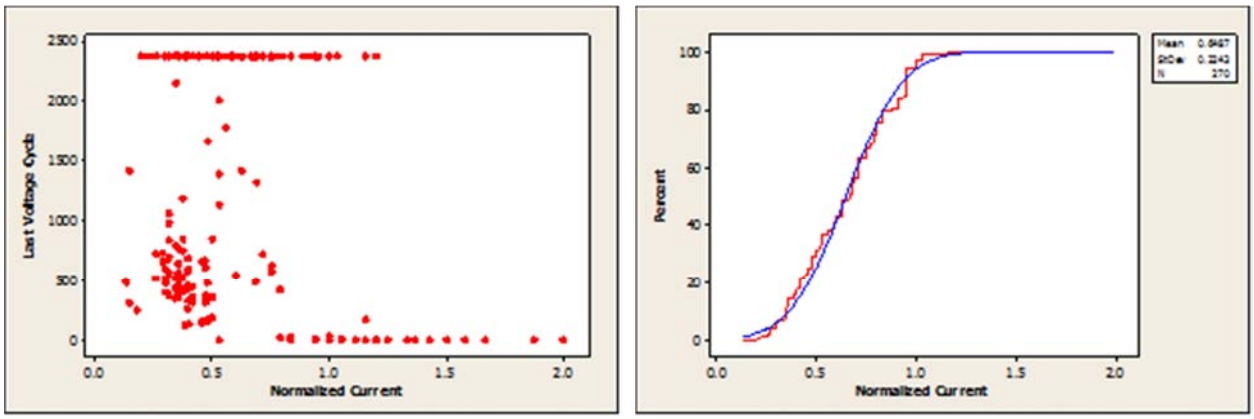

Figure 15. (*Left*) Time of last voltage half-cycle, indicating whether and/or at what time the circuit breaker removed voltage from the circuit. (*Right*) Empirical cumulative distribution function and fit of data from the circuit breakers that failed to trip during the test (*N* = 270).

Task 3 – Analysis of Ignition Hazard from Parallel Arc Faults

The energy released during an arc is the mechanism for igniting the insulation material and hence the primary concern for fire risk. Therefore, the analysis of arc energy release is conducted separately here, first through a statistical analysis of energy release, then applying this information to obtain a probability of fire using the experimental data which evaluated whether ignition had occurred during the test.

This analysis is separate from the traditional criterion of requiring an AFCI to trip within eight half-cycles per UL 1699, but is able to tie a probability of ignition if the eight half-cycle criterion is used for mitigation.

Selection of this eight half-cycle limit has been historically considered a reasonable balance of AFCI technical ability, avoidance of nuisance tripping, and ability to minimize the risk of fire due to arcing faults. This analysis is not intended to override any existing AFCI requirements or suggest that those trip thresholds require revision. In particular, the analysis included here is narrowly focused on the ignition of PVC-based wire insulation within NM cable. Residential AFCIs are required to mitigate arcing faults regardless of insulating material, as well as mitigate arcing faults within electrical appliances. Since the materials systems and circumstances of arcing faults are not likely to be known in most applications, a conservative or otherwise rigid trip threshold based on number of arcing half-cycles is appropriate. However, in the current project with a narrowly focused arcing situation, it may be appropriate to consider alternative criteria for mitigation based on probability of ignition of PVC insulation. This consideration is outside the scope of this work. However, this analysis provides scientific background on this subject should alternatives to UL 1699 requirements be considered for breaker mitigation of parallel arcing faults in NM cable. The data are also useful in assigning a probability of ignition based on tripping conditions; for example, the probability of ignition should breakers trip in one half-cycle while operating in the magnetic trip regime.

Table 5. Goodness-of-fit (*R* squared values from ANOVA) for identified independent variables influencing the energy released in each arcing half-cycle.

Variable	R-Sq (%)	R-Sq (adj) (%)	P	N
Short-Circuit Current (I_{max})	35.64	35.63	0.000	22728
Iteration Number	9.92	9.90	0.000	22728
Half-Cycle Number	16.87	9.42	0.000	22728
Breaker Magnetic Trip Level	2.07	2.02	0.000	22728
Breaker Number	1.03	1.00	0.000	22728
Manufacturer	0.74	0.73	0.000	22728
Breaker Age	0.00	0.00	0.661	22728

Arc Energy Behavior

The energy released in each arcing half-cycle was calculated by measuring the voltage and current waveforms between the strike and stop angles, and integrating with respect to time.

$$E = \int_{\theta_{Strike}}^{\theta_{Stop}} V(t) \cdot I(t)\, dt \tag{18}$$

In practice, this was done automatically by multiplying first the voltage and current sample at each instant in time, then multiplied by the duration of each sample (in this study, a sample rate of 250 kS/s was used,

so the duration of each sample was 4 μs). Each of these samples was then summed to give the total energy in Joules for each arcing event:

$$E = \sum_{n=\theta_{Strike}}^{\theta_{Stop}} V(n) \cdot I(n) \cdot \Delta t \tag{19}$$

where Δ*t* is time interval between samples, in seconds.

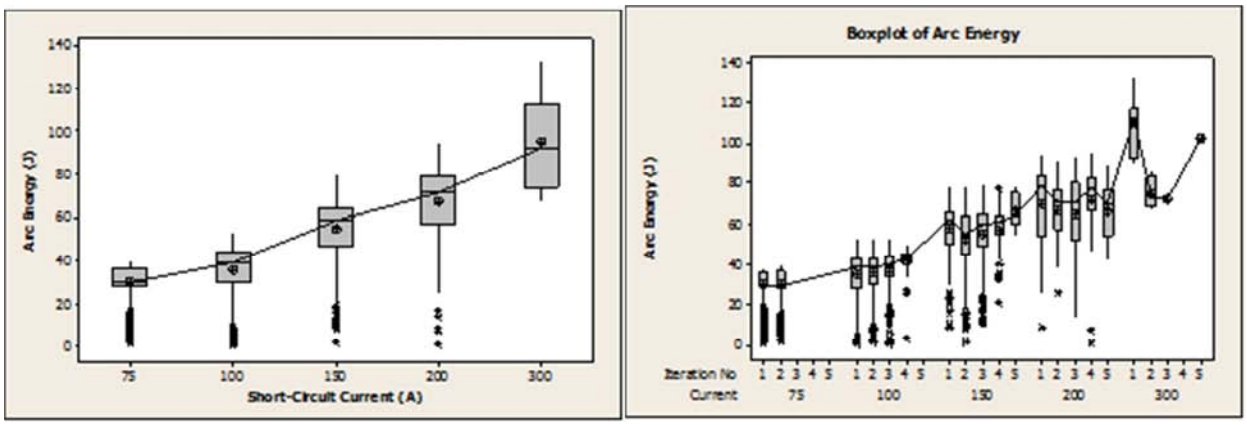

Figure 16. *(Left)* Boxplot of arc energy released each arcing half-cycle as a function of short-circuit current. *(Right)* Boxplot showing the relationship of arc energy versus iteration number, indexed to current.

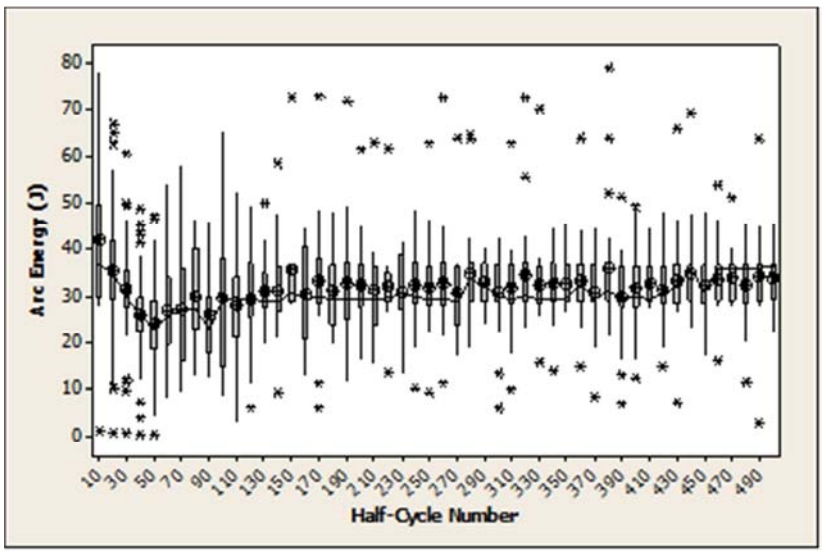

Figure 17. Boxplot showing the arc energy released in each arcing half-cycle as a function of time.

The energy released for each arcing half-cycle was then recorded and indexed to each test variable. As previously, the correlation of the arc energy can be analyzed using ANOVA to determine the relationship of the key test variables to the arc energy. Table 5 shows this analysis. In the table, *N* is the number of data points used in the statistical analysis. It is seen that the short-circuit current is the dominant variable influencing arc energy per half cycle (Figure 16, *left*). This relationship is understandable since the arc current is dominated by the short-circuit current (showing a median peak current of 0.8 times the short-circuit current, as seen in Figure 4). The independence of all other variables supports the initial conclusion that arcing generated by either a carbonized path or by a point contact will give statistically identical results. As can be seen in Figure 16 (*right*), the *R* value for iteration number is artificially inflated due to an increased number of iterations at higher short-circuit currents. The half-cycle number (Figure 17) showed a higher *R* value since at the start of the arcing event, arc energy in each half-cycles is increased, then drops to a minimum around the 50th half-cycle. As the arcing event exceeds approximately 100 half-cycles, the distribution of the arc energy reaches a steady-state.

Model for Arcing Energy

In order to use the arc energy data for estimating the probability of ignition, a generalized model of the statistical distribution of arc energy per half-cycle was developed. The ANOVA analysis identified the magnitude of arc energy is the short-circuit current (Figure 16, *left*) as a dominant variable. Therefore, an initial analysis was explored using the statistical distribution of arc energy for individual short-circuit currents. Figure 18 shows two histograms of the arc energy, at 100A and 200A. It may be observed that the shape of the probability distribution functions are the similar for each, and the magnitudes for each scale with the short-circuit current. Previous work[11] has shown that the probability distribution governing most arcing behavior is a 3-parameter log-normal distribution. The scaling of values also suggests that the energy values can be normalized relative to the short-circuit current and allow for a more generalized description of arc energy. Thus, a normalized arc energy is therefore defined as:

$$\bar{E} \equiv \frac{E}{I_{max}} \tag{20}$$

where *E* is the arc energy per half-cycle, and I_{max} is the short-circuit current. This normalized energy has units of J/A. This normalized energy is then modified by subtracting it from 1 to match a log-normal distribution. The resulting histogram and fit is shown in Figure 19 *(left)*.

In order to calculate mean and standard deviation data for the normalized energy, the data were transformed into a normal distribution. This can be done by using the transformation function as shown in Equation (21):

$$xform \equiv ln[(1 - \bar{E}) - Thresh] \tag{21}$$

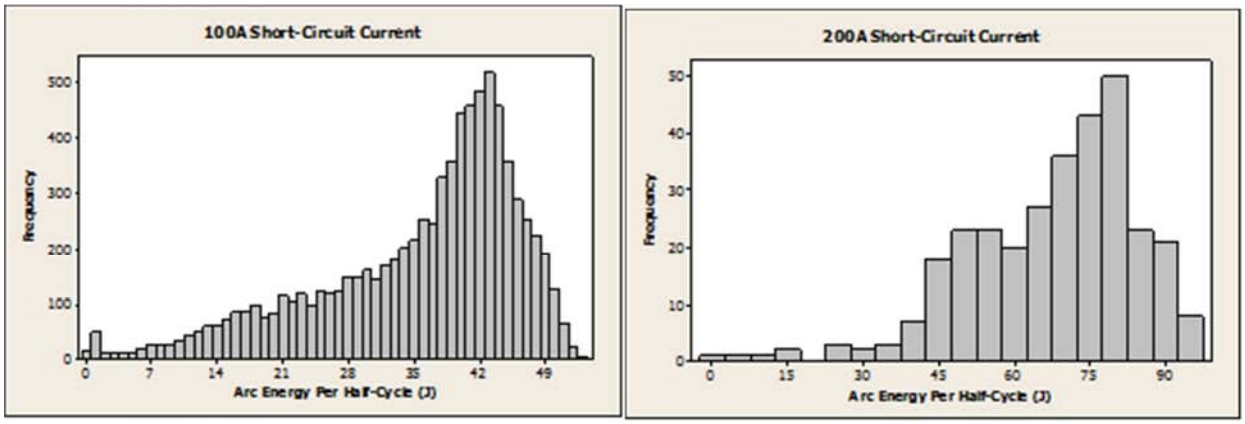

Figure 18. Histograms for arc energy per half-cycle for *(left)* 100A and *(right)* 200A short-circuit current.

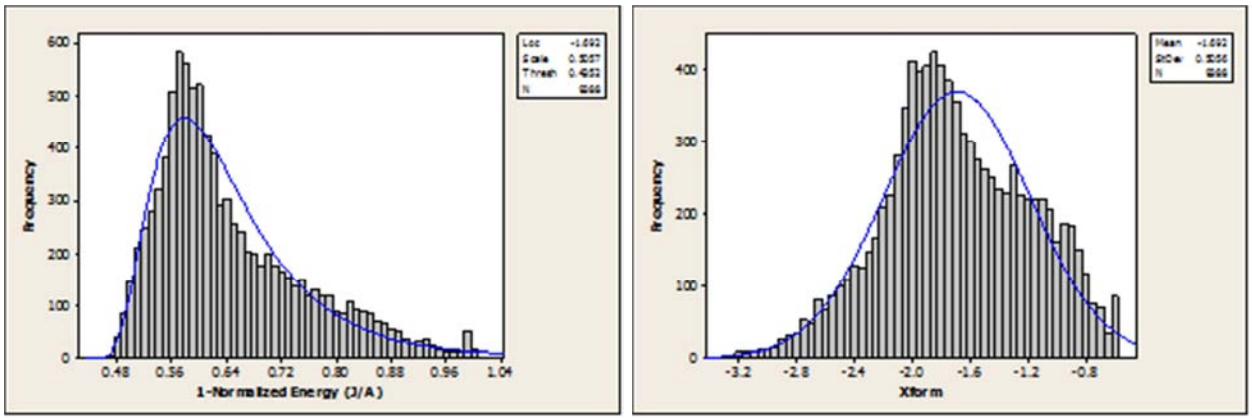

Figure 19. *(Left)* Log-normal fit of modified normalized energy at all short-circuit currents.

where *Thresh* is the threshold value from the 3-parameter log-normal fit. Figure 19 *(right)* shows a representative fit using the transformed data. From this normal distribution, the mean and standard deviation values, respectively, can be calculated by reversing the transform:

$$\overline{E_{\mu}} = Thresh + e^{xform_{\mu}} \tag{22}$$

$$\overline{E_{\pm\sigma}} = Thresh + e^{(xform_{\mu} \pm xform_{\sigma})} \tag{23}$$

Table 6. Fitting data and statistical information on the normalized energy released per half-cycle.

Short-Circuit Current (A)	Lognormal Fit Parameters			Normal Fit Parameters		Normalized Energy Distribution (J/A)		
	Loc	Scale	Thresh	Mean	Std Dev	–Std Dev	Mean	+St Dev
75[†]	–2.209	0.6559	0.4645	–2.209	0.6556	0.3240	0.4257	0.4785
100	–1.735	0.5288	0.4419	–1.735	0.5289	0.2587	0.3817	0.4542
150	–1.531	0.4257	0.3993	–1.531	0.4260	0.2695	0.3844	0.4594
200	–1.638	0.3956	0.4521	–1.638	0.3962	0.2590	0.3535	0.4171
300*	6.240	$1.3 \cdot 10^{-4}$	–512.3	6.240	$1.3 \cdot 10^{-4}$	0.3748	0.4415	0.5082
ALL	–1.692	0.5057	0.4352	–1.692	0.5056	0.2595	0.3806	0.4537

[†]The distribution at 75A exhibited two peaks rather than one. This resulted in a less-optimal fit.

*N = 13 at I_{max} = 300A, so fitting was not well correlated. Fitting was likely not accurate.

where $xform_{\mu}$ and $xform_{\sigma}$ are the mean and standard deviation values from the normal fit of the transformed data, respectively.

Table 6 shows the resulting fitting data and statistical information from fits as a function of I_{max}. Note that the 75A data exhibited two peaks rather than one, and therefore resulted in a less-optimal curve fit. The 300A data contained only 13 points, and also exhibited poor fitting. The data for 100A, 150A, 200A, and all data together show similar statistical values for the normalized energy, and suggest that a generalized model based on the normalized energy is sufficient for generalized modeling arc energy. This generalize model is expressed in the “ALL” row in the table.

Analysis of Total Arc Energy Released

Expanding now to total arc energy released per test, a similar analysis as before can be carried out evaluating the influence of test variables on total energy released. Table 7 shows the results of the ANOVA analysis. As can be seen, only the short-circuit current I_{max} has a significant influence on the total energy released (Figure 20, *left*), and will be the focus of analysis for this attribute. The iteration number can be neglected for similar reasons as has been shown previously (Figure 20, *right*).

Table 7. Goodness-of-fit (*R* squared values from ANOVA) for identified independent variables influencing the energy released in each test. *N* is number of data points used in each calculation of the *R* values. *P*-values are also given for each variable.

Variable	R-Sq (%)	R-Sq (adj) (%)	P	N
Short-Circuit Current (I_{max})	29.46	28.98	0.000	595
Iteration Number	5.32	4.68	0.000	595
Breaker Trip	0.83	0.66	0.026	595
Manufacturer	0.92	0.42	0.141	595
Breaker Age	0.19	0.02	0.286	595
Breaker Magnetic Trip Level	1.86	0.00	0.609	595
Breaker Number	0.37	0.00	0.948	595

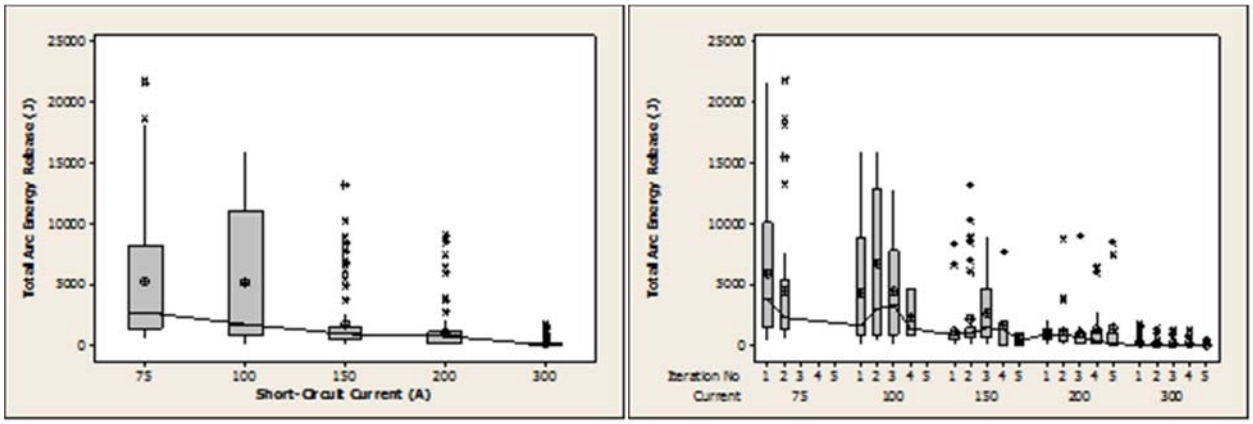

Figure 20. *(Left)* Boxplot showing total arc energy released for each test as a function of short-circuit current. *(Right)* Boxplot showing the relationship of arc energy to iteration number and short-circuit current.

Comparing the results in Figure 16 *(left)* and Figure 20 *(left)*, it is observed that though the arc energy per half-cycle increases with I_{max}, the total energy release follows the inverse relationship, with more total energy released at lower currents. This is because the circuit breaker delays tripping at lower currents longer, allowing more half-cycles to occur, while very few cycles are able to occur when the short-circuit current exceeds the magnetic trip level of the circuit breaker. As has been demonstrated previously, magnetic tripping on arcing faults is not expected to occur until the short-circuit current exceeds the magnetic trip level by a factor of 1.25. Considering this, a more meaningful relationship between total arc energy released and breaker performance would be to compare data in terms of the normalized current as before (Figure 21, *left*). This results in a scatterplot that shows a linear relationship for the upper bound of total arc energy released, which decreases towards zero energy at approximately 1.25 times the magnetic trip level, then showing energy at or near zero above this threshold.

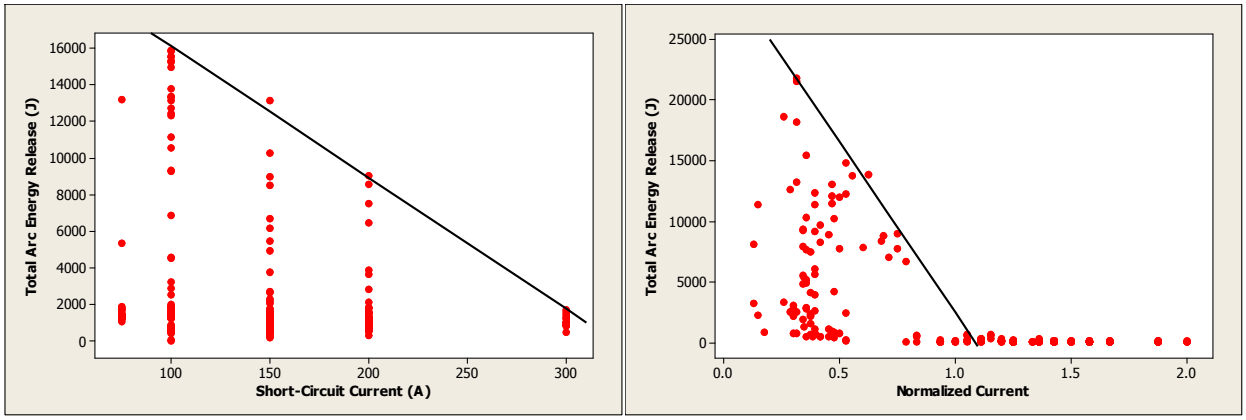

Figure 21. *(Left)* Total arcing energy as a function of short-circuit current, showing points which did not result in a breaker trip. Solid black line shows linear fit of upper bound of data. *(Right)* Total arcing energy as a function of normalized current, showing points which resulted in a breaker trip.

Observing the plots in Figure 21 suggest a linear relationship of the upper bound of total arc energy and current. Figure 21 shows two linear fits to this upper bound, one using the data where the circuit breaker tripped during the test, and one where the circuit breaker did not. The linear fit for these two data sets result in the following equations for the upper limit of the data:

$$E_{max}(I_{max}) = 23271 - 71.681 \cdot I_{max} \quad \text{(Not Tripped)} \quad (24)$$

$$E_{max}(\bar{I}_{test}) = 30563 - 28035 \cdot \bar{I}_{test} \quad \text{(Tripped)} \quad (25)$$

These two limits suggest that total arc energy can be limited by one of two mechanisms when operating below the magnetic trip level. One is thermal tripping of the circuit breaker, which may include shorting half-cycles (which tend to hasten tripping of the circuit breaker). Since this mechanism is governed by the trip level of the circuit breaker, normalized current is the governing variable in this case. A second is failure of the NM cable itself, where the circuit is opened due to the arc destroying the electrical connection of the cable or the arcing path. In this case, it is not expected that the magnetic trip level of the circuit breaker will be a factor in total energy release when the circuit breaker does not trip; therefore, the short-circuit current is used.

These two proposed linear relationships do not enable prediction of total arc energy release based on whether the circuit breaker trips, but it does place an upper bound on the total possible release of arcing energy for a given magnetic trip level and/or short-circuit current. It may be observed, that for the tripping data, the *x*-intercept is located at 1.1 times the magnetic trip level, which is reasonably consistent with the 1.25 value previously associated with breaker tripping and arcing behavior. The upper bound for the data where the circuit breaker failed to trip suggests that arc energy release will not increase without bound,

and is expected to approach zero as the short-circuit current approaches 325 A. This suggests that 14 AWG conductor used in NM cable will limit arc faults above 325 A similar to the action of a fuse, though most modern breakers will trip magnetically at or above this level (this is not the case with older breakers, which may have a magnetic trip level exceeding 325 A).

Analysis of Ignition versus Energy Release

To understand the relationship of energy release and ignition, it was recorded from each test whether ignition of the wiring insulation had occurred. The observations from each test showed clearly that there is no definitive boundary that can be easily discerned between insulation which has ignited and that which had not. Cables exhibited extreme cases of ignition, as shown in Figure 22 (the test sample above had an I_{max} of 75A), to no visible external damage at all. Therefore, “ignition” was defined for a given test if visible charring was observed on the surface of the insulation of the NM cable. The assumption was that if the outer insulation jacket showed signs of combustion, there was a significant probability of ignition of materials surrounding the cable. This is a conservative approach to identifying a lower threshold for ignition.

Figure 22. Photograph of a test sample exhibiting extensive damage from cable ignition. Samples exhibited a continuum of damage, from heavily damaged (as above) to visibly undamaged.

Table 8. Goodness-of-fit (*R* squared values from ANOVA) for identified independent variables which show correlation to the observed ignition in each test.

Variable	R-Sq (%)	R-Sq (adj) (%)	P	N
Total Arc Energy Release	27.61	27.34	0.000	274
Last Arcing Half-Cycle	24.77	24.50	0.000	274
Number Arcing Half-Cycles	23.61	23.33	0.000	274
Last Shorting Half-Cycle	20.77	20.48	0.000	274
Iteration Number	4.51	4.16	0.000	274
Breaker Number	0.82	0.45	0.136	274
Normalized Current	0.57	0.21	0.211	274
Short-Circuit Current (I_{max})	0.17	0.00	0.500	274
Last Voltage Half-Cycle	0.10	0.00	0.611	274
Test Number	0.01	0.00	0.875	274
Breaker Magnetic Trip Level	0.01	0.00	0.852	274
Number of Shorting Half-Cycles	0.00	0.00	0.964	274

In Table 8, *N* is number of data points used in each calculation of the *R* values. *P*-values are also given for each variable.

An ANOVA analysis of the ignition data is shown in Table 8. The analysis suggests that the total arc energy is the dominant factor influencing ignition. It is noted that other factors have a similar level of influence, however, variables such as the number of arcing half-cycles and the time of the last arc half-cycle are closely related to energy release, and therefore reflect the relationship of energy release and ignition. The correlation to the last shorting half-cycle is not clear, but may be somehow tied to the total duration of the event, where a shorting half-cycle occurs after a time of arcing. It appears that shorting in itself was not a factor in ignition, which is reflected by the lack of correlation of the number of shorting half-cycles to ignition. It is noted that energy, and not current magnitude, is the factor most influencing ignition.

If heat loss with time was a significant factor influencing total energy required for ignition, it would be expected that lower power levels would tend to show a lower propensity for ignition for a given amount of energy. Since this was not observed, it can be assumed that heat loss with time is insignificant and can be neglected.

Since ignition is primarily governed by total energy release, it is important to characterize this to determine a lower bound on the amount of energy that is expected to lead to a high probability of ignition. Figure 23 (*right*) shows energy release per half-cycle, which can be treated as an indicator of power. This power plot shows no relationship to ignition, suggesting that the power magnitude is less important than the time it is applied. If energy alone is the dominant factor, it implies that the time to ignition is small compared to the rate of heat loss to the air and through the copper conductors. An ability to neglect heat loss reduces a potentially complex dynamic model to a simplified model of total energy applied and

ignition potential. This dependence solely on total energy applied without a significant dependence on time (for very short ignition times, as is observed here) was also observed during development of UL 1699B, which cites a maximum threshold of 750 J before there is a 5% probability of ignition.[14]

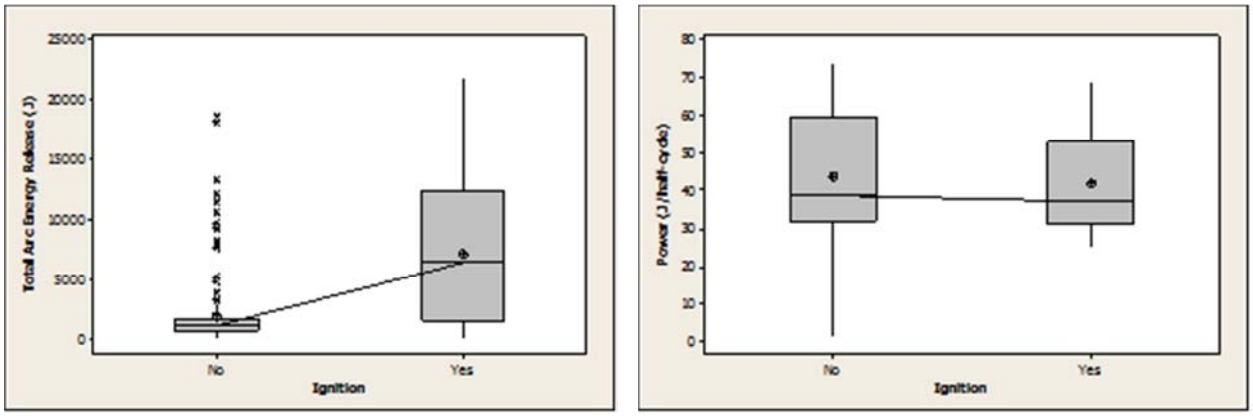

Figure 23. (*Left*) Boxplot of total arc energy released versus whether ignition occurred, which suggests an energy threshold above which ignition becomes likely. (*Right*) Boxplot of arc power (in units of Joules per half cycle) versus ignition.

If the timeframe of energy application can be neglected, a predictor of ignition can be based on an absolute threshold of energy released. Figure 24 (*left*) shows two empirical cumulative distribution functions (CDFs) of energy release data, divided by whether ignition was observed. A three-parameter lognormal distribution appears to show the best agreement to the distribution data. To compare the distributions of the two data sets, the CDF for non-ignition is inverted and plotted with the ignition CDF, as shown in Figure 24 (*right*). The CDFs cross at 2200 J, which suggests a potential threshold for ignition. A more conservative alternative would be at 5% probability of ignition, with a total energy release of 490 J.

[14] UL Subject 1699B, "Outline of Investigation for Photovoltaic (PV) DC Arc-Fault Circuit Protection," Section 23.3.1e. April 29, 2011.

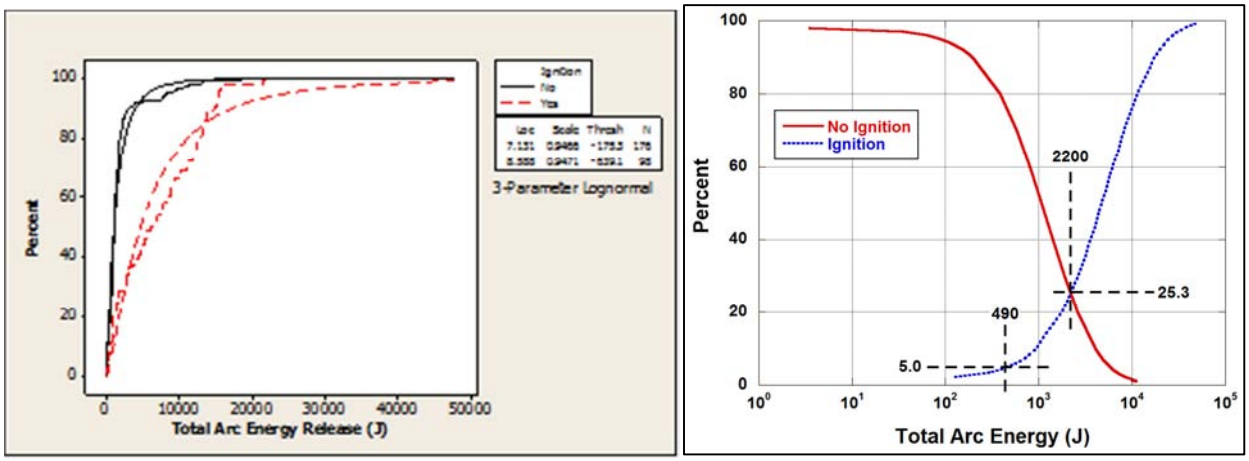

Figure 24. (*Left*) Empirical cumulative distribution functions (CDFs) of total energy released and ignition. (*Right*) Cumulative CDF fits from (*left*), comparing data from samples showing ignition to those that did not. Numbers show coordinates for 5% probability of ignition and point where the CDFs cross.

This result now can be compared to the statistical information from energy release to evaluate the probability of ignition when a breaker is utilized for mitigating a parallel arc event. Determining a specific number of “half cycles” that will directly result in ignition is not possible, since the amount of energy released in a half cycle is governed by a random process (characterized in Figure 19 and Table 6). However, a range of the probability of ignition can be calculated based on a mean energy and standard deviation values for a given number of half-cycles. This calculation is shown in Table 9: color coding in Table 9 is the same as used previously for tabulation of *R* values, *e.g.*, see Table 23. Probabilities assume that all arcing half-cycles contain the total energy as shown. Energy loss through conduction and convection mechanisms is neglected, but has been shown to be negligible for the time durations shown.

For each calculation, the total energy is assumed to be equivalent to the mean or one standard deviation above or below the mean for all half-cycles. The probability of ignition is then interpolated from the CDF shown in Figure 24. The results show that a very low probability of ignition (less than 3%) exists if the circuit breaker trips magnetically. It is also shown that very good protection is obtained if the number of arcing half-cycles is maintained at or below eight. However, reliance on breaker protection in the thermal trip regime (where the number of arcing half-cycles grows large) is shown not to be effective at preventing ignition of the cable, since probability of ignition rises quickly with the number of arcing half-cycles.

Table 9. Calculation of the probability of ignition, using the statistical model for normalized energy (Figure 19) and the empirical CDF for ignition data (Figure 24).

No. Arcing Half-Cycles	Assumed Magnitude Distribution	Estimated Total Energy Release (J)					Probability of Ignition, %				
		75	100	150	200	300	75	100	150	200	300
1	–Std Dev	24.3	25.9	40.4	51.8	112	1.3	1.3	1.4	1.5	1.9
	Mean	31.9	38.2	57.7	70.7	133	1.3	1.4	1.5	1.6	2.0
	+Std Dev	35.9	45.4	68.9	83.4	153	1.4	1.4	1.6	1.7	2.2
2	–Std Dev	48.6	51.8	80.8	104	224	1.5	1.5	1.7	1.8	2.7
	Mean	63.8	76.4	115	141	266	1.6	1.6	1.9	2.1	3.0
	+Std Dev	71.8	90.8	138	167	306	1.6	1.7	2.1	2.3	3.3
3	–Std Dev	72.9	77.7	121	155	336	1.6	1.7	2.0	2.2	3.6
	Mean	95.7	115	173	212	399	1.8	1.9	2.3	2.6	4.1
	+Std Dev	108	136	207	250	459	1.9	2.1	2.6	2.9	4.7
4	–Std Dev	97.2	104	162	207	448	1.8	1.8	2.2	2.6	4.6
	Mean	128	153	231	283	532	2.0	2.2	2.7	3.1	5.4
	+Std Dev	144	182	276	334	612	2.1	2.4	3.1	3.6	6.2
5	–Std Dev	122	130	202	259	560	2.0	2.0	2.5	3.0	5.7
	Mean	160	191	289	354	665	2.2	2.4	3.2	3.7	6.8
	+Std Dev	180	227	345	417	765	2.4	2.7	3.7	4.3	7.8
6	–Std Dev	146	155	242	311	672	2.1	2.2	2.8	3.4	6.8
	Mean	191	229	346	424	798	2.4	2.7	3.7	4.4	8.2
	+Std Dev	215	272	413	500	918	2.6	3.1	4.3	5.1	9.6
7	–Std Dev	170	181	283	363	784	2.3	2.4	3.1	3.8	8.0
	Mean	223	267	404	495	931	2.7	3.0	4.2	5.0	9.7
	+Std Dev	251	318	482	584	1071	2.9	3.4	4.9	5.9	11
8	–Std Dev	194	207	323	414	896	2.5	2.6	3.5	4.3	9.3
	Mean	255	306	462	566	1064	2.9	3.3	4.7	5.7	11
	+Std Dev	287	363	551	667	1224	3.2	3.8	5.6	6.8	13
10	–Std Dev	243	259	404	518	1120	2.8	3.0	4.2	5.3	12
	Mean	319	382	577	707	1330	3.4	4.0	5.8	7.2	15
	+Std Dev	359	454	689	834	1530	3.8	4.6	7.0	8.6	17
15	–Std Dev	365	389	606	777	1680	3.8	4.0	6.1	8.0	19
	Mean	479	573	866	1061	1995	4.9	5.8	9.0	11	23
	+Std Dev	539	681	1034	1251	2295	5.5	6.9	11	14	26
20	–Std Dev	486	518	808	1036	2240	4.9	5.3	8.3	11	25
	Mean	638	764	1154	1414	2660	6.5	7.8	12	16	30
	+Std Dev	718	908	1378	1668	3060	7.3	9.4	15	19	35
30	–Std Dev	729	777	1212	1554	3360	7.4	8.0	13	17	38
	Mean	957	1146	1731	2121	3990	10	12	19	24	44
	+Std Dev	1077	1362	2067	2502	4590	11	15	23	29	49
50	–Std Dev	1215	1295	2020	2590	5600	13	14	23	30	56
	Mean	1595	1910	2885	3535	6650	18	22	33	40	63
	+Std Dev	1795	2270	3445	4170	7650	20	26	39	45	68

Task 4 – Summary of Findings

Circuit Breaker Characterization

Despite rejection of the EIA proposal for the 1996 NEC, circuit breakers evaluated in this work demonstrated magnetic trip levels consistent with the 1996 recommendations, showing a mean magnetic trip level of 213A (Figure 7), which correlates well with Franklin's observation that average arcing magnitudes are expected to be "around 200 to 250 Amperes".[9]

Considering the literature and the experimental results here, it appears that the "new" breaker data cited in this work is representative of circuit breakers currently manufactured, perhaps as well as breakers in service for the past 10 or 20 years, presumably during or after the 1996 EIA proposal, or at least after the Franklin publications. Therefore, results from this work based on "new" breaker data is expected to match most real-world installations. However, the "old" breaker data may or may not be representative of a specific older installation. Since breaker magnetic trip levels ranged over such a wide range prior to the 1990s, it is not realistic to state a "representative" data set of old breakers and report "expected" results. However, a small sampling of older breakers was used in this work (but not analyzed) to attempt to build a wider picture of overall breaker behavior. As the ANOVA results typically show, the age of the circuit breaker does not influence behavior, even if the "old" breakers are included in the analysis. (See Table 15 and Table 23, where R_{sq}(adj) is always below 3% for all test variables, which can be considered statistically unimportant.) Normalizing breaker performance to magnetic trip level therefore statistically eliminates any difference in breaker performance, allowing both old and new breakers to be validly combined together for analysis.

These reported findings and actions, however, are not in line with 2009 research work conducted at UL[11] that showed that arc current tends to have current magnitudes approximately 80% of short-circuit current, regardless of short-circuit current level. This was experimentally demonstrated to be true throughout the full range of test currents used in that study (5A to 400A). Therefore, it is reasonable to speculate that Franklin is referring to parallel arcing faults in some sampling of real-world systems, implying that short-circuit currents are not expected to fall below 120A. However, UL Standard 1699 requires AFCI testing at 75A short-circuit current, which is typically achieved by the addition of lengths of NM cable (typically 200-300 feet of 14 AWG cable). As the run length of branch service is not limited by Code, it is therefore possible to experience parallel arcing faults at or below 100A. In very large residences, a home run of 200-300 feet or more is possible, especially if a circuit is located at a site very remote to the service panel. At least, no part of the Code, nor any known trade practices exist which is intended to maintain a minimum short-circuit current. Therefore, a blanket assumption that arcing faults are "never" below 200A may result in safety concerns. While possibly a rare condition, insufficient data exists to determine a reasonable lower limit to available fault current that applies to *any* circuit in any residence, business, or other structure.

Arcing Response

The concerns of nuisance tripping from "low magnetic trip breakers" resulted in further research[15] and eventual industry development of the arc fault circuit interrupter (AFCI), which introduced more intelligent discrimination of arcing faults from other "normal" transients and loads. By the 1999 NEC AFCI technology began to be required for bedrooms (with an effective date of 2002),[16] expanding requirements to most residential locations by the 2008 NEC. Performance of AFCIs is evaluated by UL Standard 1699, evaluating reaction to arcing faults, as well as nuisance events such as transients and normal loads with waveforms reminiscent of arcing. For arcing faults, one key criterion for AFCI performance is reacting within eight half-cycles. This criterion appears to be a reasonable balance of AFCI ability to detect arcs, minimizing nuisance tripping, and maximizing protection against fire. However, this criterion does not appear to be directly tied to energy release and ignition modeling, at least not at its inception. However, the ignition modeling conducted in this work (Table 9) shows that eight half-cycles gives reasonably good protection from ignition, roughly 10% probability for up to 300A, and lower short-circuit currents at or below 5% probability of ignition.

The empirical analysis of circuit breaker performance, which evaluates half-cycle count against the eight half-cycle UL 1699 criterion, shows that a breaker will fail to mitigate the arc in eight half-cycles when the fault current is below the magnetic trip level of the circuit breaker. However, once the fault current exceeds the magnetic trip level of the circuit breaker, it is a near certainty that the circuit breaker will mitigate the fault in less than eight half-cycles. Table 3 shows this statistically, where at 200A there is an 88% probability that a breaker will fail to trip in eight half-cycles, where at 300A, the probability drops to 0.01%. Considering that the average breaker magnetic trip level is 213A, this shows the difference in performance below and above the magnetic trip level. Therefore, *provided an available fault current can be **guaranteed** to exceed the magnetic trip level*, breakers can be effective at mitigating arcing faults.

The discussion now turns to the statistical analysis based on data normalized so that breaker performance can be more accurately assessed between individual breakers that possess different magnetic trip levels. As it has been shown that breaker reaction to arcing faults is critically dependent on the magnetic trip level, normalization allows all breakers in this work to be compared operating in the same regime. Figure 8 shows how this normalization makes breaker performance uniform among manufacturers and age. This is also justified statistically, since only the short-circuit current was found to be a test variable of significance governing breaker performance to arcing faults (Table 23). As the empirical analysis had suggested, the statistical analysis concludes that the magnetic trip level needs to be exceeded by a factor of 1.25 to mitigate the arc within eight half-cycles (Figure 14, *left*). Furthermore, a breaker only has a 95% probability of tripping at all during an arcing event if the short-circuit current equals the magnetic trip level of the circuit breaker. Probability of a breaker trip exceeds 99% only once

[15] P. Boden *et al*., "Technology for Detecting and Monitoring Conditions that Could Cause Electrical Wiring System Fires" UL research report to the CPSC (Contract Number CPSC-C-94-1112), 1995.
[16] NFPA 70, 1999 National Electrical Code, Section 210-12, Arc-Fault Circuit-Interrupter Protection.

the short-circuit current exceeds the magnetic trip level by a factor of 1.25 (since the magnitude of an arc typically is 80% of the short-circuit current). Therefore, the previous statement about breaker effectiveness is further qualified by stating that breakers can be effective at mitigating arcing faults, *provided the available fault current can be guaranteed to exceed the magnetic trip level of the circuit breaker by a factor of 1.25*.

At this point in the analysis the circuit breaker performance is stated in general terms relative to the magnetic trip level and available short-circuit currents of the circuit. The question of exactly what short-circuit current can be expected has not yet been addressed. Assuming the available current at the panel is large (with residential service short-circuit current typically limited to 5 kA by the public utility), available current to the first receptacle in a circuit is primarily limited by the resistance of the cabling (assumed to be 14 AWG NM cable in this work). Further assuming uniform resistivity of the cable, available current therefore is governed by the length of the cable from the panel to the first receptacle (the "home run"). Studies to evaluate the range of available fault current therefore attempt to investigate the statistical distribution of home run length, or at minimum attempt to find the longest run to identify a lower bound on short-circuit current. A study by Parks Associates[17] sought to measure run lengths in homes during construction. This study however underestimated the length of home runs by assuming that all run lengths exceeding 50 feet were 50 feet. This had the effect of lowering the average run length and artificially inflating the available short-circuit current. Therefore, these results are not useful in evaluating the prevalence of extremely long run lengths, particularly those that may result in short circuit currents below 266A (the mean magnetic trip value of new breakers times the 1.25 factor for arcing faults: 213A x 1.25). Assuming a typical value of 2.53 mΩ/ft for 14 AWG wire (at 25℃), approximately 179 fe et of 14 AWG cable would result in a 266A short-circuit current. This would translate to a fault located 90 feet from the panel board. The maximum length of 50 feet artificially puts a lower bound of 475A on the short-circuit current (again assuming 100 feet total circuit length, 120 V_{rms} voltage supply, and 14 AWG cable for both hot and neutral conductors).

These results suggest therefore that provided a breaker's magnetic trip level is matched to the impedance of the home run, a breaker is expected to trip within the eight half-cycles required by UL 1699. This suggests a relationship where wire run length, gauge, and magnetic trip level are combined into a governing equation. A similar approach was reported by Packard,[18] citing a maximum allowable home run impedance (this was exhibited by a specific example assuming 12 AWG cable, and a 20 A breaker with a magnetic trip level of 240 A). First, it is known from the experimental work that to exceed a 99% probability that a breaker will trip on an arcing fault, the short-circuit current must exceed the magnetic trip level of the circuit breaker by a factor of 1.25:

[17] B. Ablondi, "AFCI Code Change Analysis Electrician's Survey," Presentation to AFCI Consortium, September 2009.
[18] T. Packard, "Analysis of Circuit Breaker Protection of the Branch Circuit 'Home Run'," Code Panel submission by Hubbell Incorporated (Delaware), Cooper Wiring Devices, Leviton Manufacturing Company, and Pass & Seymour/Legrand.

$$\frac{I_{max}}{I_{mag}} > 1.25 \tag{26}$$

Solving for I_{mag},

$$I_{mag} < \frac{I_{max}}{1.25} \tag{27}$$

The short-circuit current is related to the wire impedance and supply voltage by Ohm's Law:

$$V_{rms} = I_{max} \cdot R \tag{28}$$

The resistance *R* is governed by the resistivity of the cable:

$$R = 2\rho_L L \tag{29}$$

where *L* is the length of the home run in feet and ρ_L is the resistivity of the cable in ohms/foot. The factor of 2 is added to incorporate the resistance of the supply and return cables (this assumes the return path is of the same wire gauge as the supply gauge, generally true for NM cable). Combining these equations results in the inequality:

$$I_{mag} < 0.4 \cdot \frac{V_{rms}}{\rho_L L} \tag{30}$$

Since the magnetic trip of the circuit breaker may be an uncontrollable variable, a more convenient relationship may be in terms of run length and wire gauge:

$$\rho_L L < 0.4 \cdot \frac{V_{rms}}{I_{mag}} \tag{31}$$

Therefore, to ensure protection from parallel faults in the NM cable from the circuit breaker, the wire gauge and/or the run length is adjusted so that sufficient fault current is available anywhere in the run. Note that the value for *R* in this inequality neglects any output impedance from the panel, which generally is a reasonable approximation. If this is not the case, the value for *R* above needs an additional term to incorporate the available current of the panel:

$$R = 2\rho_L L + \frac{V_{rms}}{I_{pssc}} \tag{32}$$

where I_{pssc} is the available short circuit current at the panel.

Unless the magnetic trip level of the individual breaker is characterized, it is not typically a known value. Therefore, though a more conservative approach, the statistical information as shown in Figure 7 can be

leveraged to determine the highest expected magnetic trip level for most newer breakers (manufactured after the year 1995 or so). This approach is not recommended for older breakers, since it is known that the magnetic trip level can vary considerably. In older installations, it would likely be necessary to characterize the circuit breaker's magnetic trip level, or replace the old breaker with a newer model. In the case of a new breaker, it was found that the average magnetic trip level was 213 A with a standard deviation of 33.2 A. To ensure that the available current exceeds the magnetic trip level of 99% of all breakers in the field, a magnetic trip level of 299 A is used. (This is calculated using 2.576 standard deviations, which corresponds to a 99% probability, added to the mean of 213 A.) In this instance, the value for the home run impedance is the following:

$$\rho_L L < 0.4 \cdot \frac{120}{299} = 161\ m\Omega \tag{33}$$

As the resistance of a cable will change with temperature, a worst-case scenario would be to assume this maximum allowable impedance (161 mΩ) at the maximum operating temperature allowed for most residential wiring (typically 90℃), since the leng th of cable will have its largest resistance at this temperature. It is noted that cable resistance per unit length is usually listed in the literature at 25℃ (room temperature). Conversion between resistances can be accomplished using the following expression:

$$T_2 = \frac{R_2}{R_1}(k + T_1) - k \tag{34}$$

where R_2 is the resistance at temperature T_2, R_1 is the resistance at temperature T_1, and k is the coefficient of resistance (for copper, k is equal to 234.5℃). Using this formula to solve for R_2, the equivalent resistance at 25℃ can be determined to ensure the cable resistance will be equal to 161 mΩ at 90℃:

$$25 = \frac{R_2}{0.161}(234.5 + 90) - 234.5 \tag{35}$$

Solving for R_2 gives a resistance of 128 mΩ at 25℃. Assuming 14 AWG wire (ρ_L = 2.575 mΩ/foot at 25℃), this would suggest a maximum home run length L of 50 feet. This maximum value would be further reduced if the output impedance of the panel is not much greater than the impedance of the run length.

This inequality now sets conditions so that 99% of all breakers (assuming they are of the "new" type) will have a 99% probability of magnetically tripping on a parallel arcing fault. Though this suggests a high level of protection, significant energy is still being released as an arcing fault. Assuming that the home run impedance was set so that the arcing fault was 300A, Table 9 shows that the probability of ignition for a single half-cycle is estimated at 1.9 to 2.2 percent. Therefore, it is expected that in 98% of all parallel arcing conditions mitigated in this way will not result in ignition of the insulation material. In the event that additional half-cycles are allowed to pass before the circuit breaker trips, each additional half-cycle adds roughly one additional percent to the probability of ignition. Therefore, provided the necessary conditions

described here apply, a home run and breaker can be matched so that it will trip on 99% of all parallel arcing faults within a single half-cycle, resulting in a 2% probability of ignition.

Conclusions

The following conclusions are now made concerning an ability of a circuit breaker to mitigate a parallel arcing fault in lieu of a panel-mounted AFCI:

- New circuit breakers show an average magnetic trip level of 213A, with a standard deviation of 33.2A. This suggests that 99% of all circuit breakers will possess a magnetic trip level at or below 300A. This is true for all brands of circuit breakers investigated in this work.
- Arcing behavior (with respect to strike angle, peak current, etc.) is not influenced by the circuit breaker itself. Therefore, the results in this work apply to all types of arcing, including carbonized path and point contact arcing.
- A circuit breaker will give adequate protection from parallel arcing (as defined by UL 1699) provided that the short-circuit current exceeds the magnetic trip level of the circuit breaker by a factor of 1.25.
- A circuit breaker is expected to provide protection from a parallel arcing fault when the following inequality is satisfied:

$$\rho_L L < 0.4 \cdot \frac{V_{rms}}{I_{mag}}$$

  where L is the NM cable run length in feet, ρ_L is resistance of the conductor in ohms per foot, V_{rms} is the circuit voltage, and I_{mag} is the magnetic trip level of the circuit breaker. This inequality assumes that the available current at the panel is much greater than I_{mag}.
- Assuming a 15A, 120 V_{rms} circuit using 14AWG NM cable for the home run, a new circuit breaker will provide protection from a parallel arcing fault if the run length does not exceed 50 feet. This assumes a maximum allowable operating temperature of 90℃.
- Assuming a 300A fault current and satisfying the inequality above, the probability of ignition of the cable during an arcing event is 2% if a circuit breaker trips in one half-cycle, this probability of ignition increasing by 1% for each additional half-cycle of arcing.

Appendix A: Analysis of Arcing Behavior

Prior to analyzing the behavior of circuit breakers in response to parallel arcing faults, it is desirable to understand the influence of test variables on the generated arcing behavior. The goal in this section is to determine whether arcing can be considered as an event independent of circuit breaker-related test variables, or whether changes in arcing behavior need to be linked to both breaker test parameters and breaker performance. An ability to prove statistical independence of arcing behavior from test parameters will simplify the final analysis of circuit breaker performance during arcing events. This analysis is conducted using the ANOVA method of analysis. Five key arcing attributes are analyzed here with respect to several test variables. This information will determine whether all generated arcing is uniform for all tests, or whether specific test variables alter arcing behavior.

Analysis of Normalized Peak Current

The peak current is defined in this study as the largest magnitude of current measured within each half-cycle of the waveform. These points were collected automatically using LabVIEW-based software and tabulated with corresponding variables, such as the half-cycle number, circuit breaker manufacturer, age of the circuit breaker, etc. To allow for a useful comparison of data from all tests, a normalized peak current was defined and calculated as:

$$\bar{I}_{peak} \equiv \frac{\left|I_{peak}\right|}{\left|I_{\max}\right|} = \frac{\sqrt{2}}{2} \cdot \frac{\left|I_{peak}\right|}{\left|I_{\max(rms)}\right|} \tag{36}$$

Three states of behavior were observed for peak current values: arcing behavior, non-arcing behavior, and shorted. Each of these three modes of behavior was segregated by defining two current thresholds relative to the short-circuit current I_{max} (Figure 25). A threshold of 20% I_{max} was defined as the minimum for arcing behavior. Selection of this value can be considered somewhat arbitrary, and does not follow what is defined in UL 1699 for minimum arcing (which is defined as 5% of I_{max} in the standard). However, a very low value for the threshold, such as 5%, often would be within the large number of insignificant events (very short-duration arcing, noise, etc.) and were not likely to contribute to the understanding of the arcing behavior. At 20% I_{max} a very small percentage of data points were typically found and was a convenient threshold for defining a threshold for arcing. As this was within a “long tail” of the probability distribution function, moving this threshold ±10% in either direction would have a negligible effect on the total number of points included and therefore not affect the analysis.

The relative influence of each variable on the normalized current was analyzed using ANOVA, and evaluated according to the resulting adjusted *R* squared ($R_{sq}(adj)$) values. Table 10 summarizes the degree of influence each independent variable has on the normalized peak current. Larger $R_{sq}(adj)$ values

mean that the variable has a larger influence on the peak current, with 100 meaning complete influence, and 0 denoting no influence. Defining "significance" is difficult, but $R_{sq}(adj)$ values exceeding 5 or 10 percent can be considered to have influence that needs to be evaluated further. As is seen in Table 10, I_{max} and cycle number have $R_{sq}(adj)$ values greater than 10%, and therefore require a more in-depth assessment of their influence on the peak current (Figure 26). The average normalized current falls with increased short-circuit current, a result that was also found in an earlier study.[19] In this study it was also found that the average normalized current is lower during the first few half-cycles, increasing to approximately 0.9 of short-circuit current. The magnitude of normalized current gradually falls with time, due to the heating of the wiring and therefore increase in the resistance of the circuit.

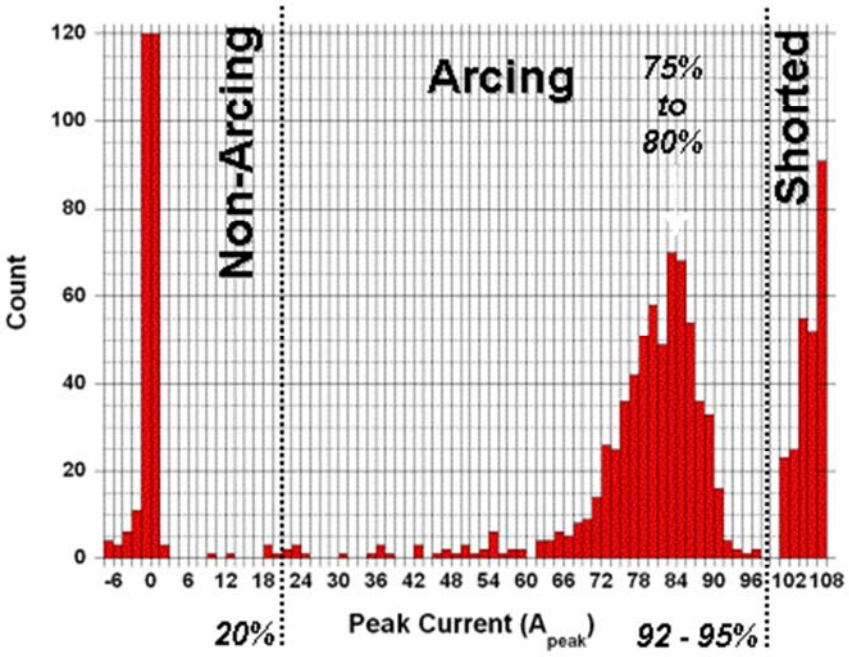

Figure 25. Representative probability distribution function for all peak current values from one series of tests, showing three modes of behavior: non-arcing (<20% I_{peak}), arcing (20% < I_{peak} < 92%-95%), and shorting (>92% to 95% I_{peak}). From Ref. 19.

[19] P.W. Brazis et al., "Synthetic Arc Generator for UL1699, Phase 2: Statistical Characterization of Arc Fault Behavior," *UL Internal Report*, 2009.

Table 10. Goodness-of-fit (*R* squared values from ANOVA) for identified independent variables influencing the value of normalized peak current during arcing events. *N* is number of data points used in each calculation of the *R* values. *P*-values are also given for each variable.[20]

Variable	R-Sq (%)	R-Sq (adj) (%)	P	N
Short-Circuit Current (I_{max})	18.55	18.54	0.000	40212
Cycle Number	15.84	11.85	0.000	40212
Iteration Number	4.10	4.09	0.000	40212
Breaker Number	1.06	1.04	0.000	40212
Manufacturer	0.91	0.90	0.000	40212
Breaker Age	0.04	0.04	0.000	40212

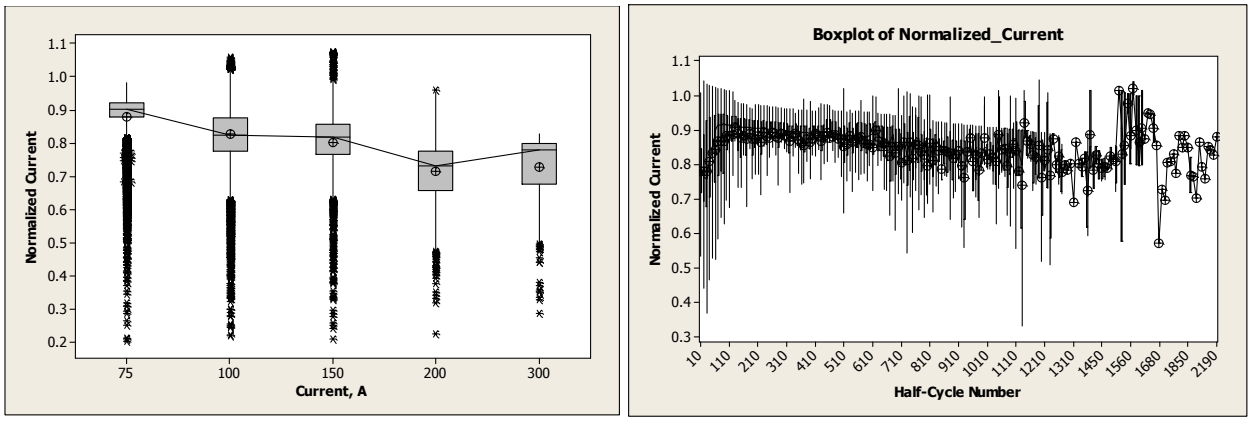

Figure 26. Boxplots for *(left)* normalized current as a function of available current and *(right)* as a function of half-cycle number.

Analysis of Phase Data

This section analyzes the point in time within each half-cycle (measured in phase angle, as defined previously in the section "Terminology") arcing begins and ends, as well as the corresponding voltage measured as these points in time. Strike and stop angle are detected automatically using LabVIEW software that analyzes each arcing half-cycle of the current waveform, digitally filtered to include components between 10 kHz and 100 kHz. (This is intended to be a high-pass signal, but in practice a bandpass signal is used to minimize aliasing effects.) The point where this signal is at its highest magnitude is recorded (in terms of phase angle, relative to the zero crossings of the voltage waveform). Two maxima are recorded, one before the peak current value and one after, each assumed to be the

[20] A *P*-value less than 0.05 indicates a statistically significant relationship. The *P*-value can be considered a measure of the signal-to-noise ratio for a given variable, with a low *P*-value suggesting that there is sufficient "resolution" to view the influence of one variable on another.

strike and stop angles, respectively (Figure 27). Detection relies on the assumption that the discontinuity in the current waveform caused by the strike and stop of the arcing event generates a large wideband signal.

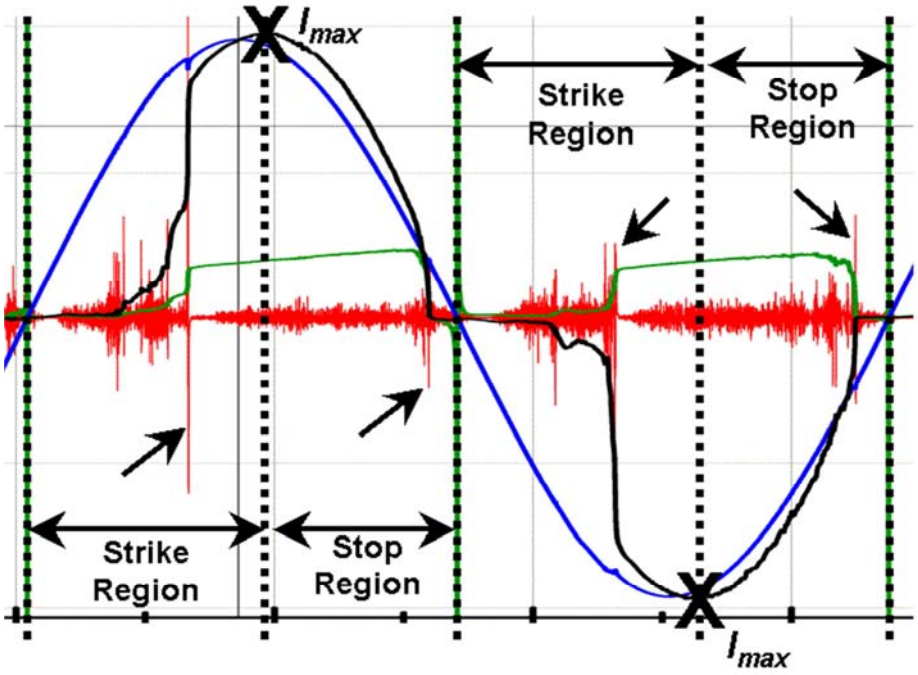

Figure 27. Schematic showing extraction of phase data. Strike and stop regions are assumed to be before and after I_{max}, respectively. In each region the maximum value is found in the high-pass filtered current waveform data (shown in red). Arrows mark the locations of the extracted strike and stop data. Note that often the voltage waveform (shown in blue) often drops at these points.

The strike and stop voltage are collected by recording the measured voltage magnitude at the same instant in time as the strike and stop phase angle. Though in theory the strike voltage should be related to the sine of the phase angle, in reality it varies depending on the impedance of the circuit and the arcing event. Therefore, the recorded voltage will often be lower than the unloaded supply voltage:

$$v_{strike}(t) \le V_{peak} \sin(\theta_{strike}),\ v_{stop}(t) \le V_{peak} \sin(\theta_{stop}) \tag{37}$$

Therefore, these two inequalities can be utilized for error checking of the phase data values, which may be incorrect due to errors in detecting the strike and stop phase angle, or misalignment of the voltage and current waveforms. Therefore, for analysis data are used only if both inequalities above are true (since a voltage outside these ranges suggests an error is highly probable). Figure 28 shows the phase angle

versus voltage relationship of the collected data and the effect of filtering. Eliminating only data with impossible voltage values, *i.e.*, voltages exceeding that of the open-circuit supply, also minimizes other issues, including unexpectedly low voltages, improbably early stop phase angle, etc.

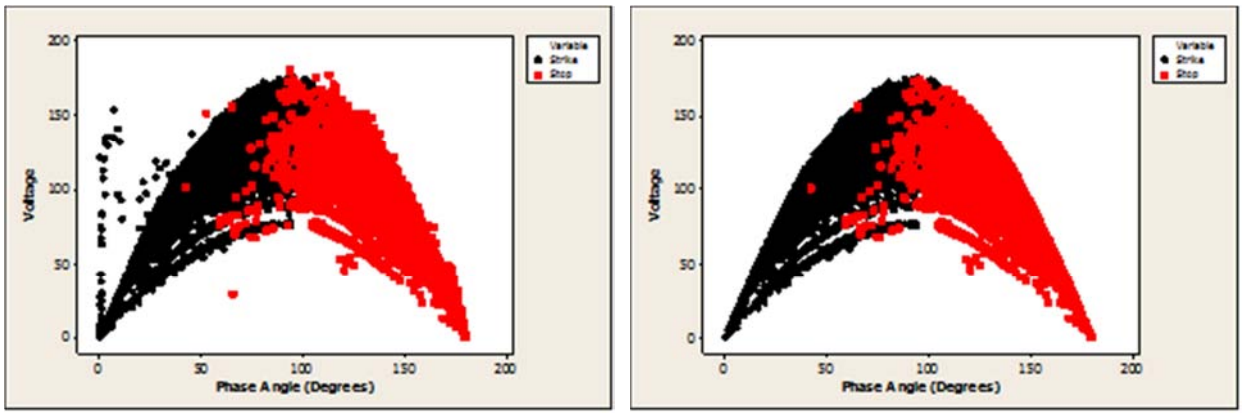

Figure 28. Effect of filtering on the phase data. *(Left)* Unfiltered data, showing various issues such as unexpectedly high and low voltage relative to phase angle and very early stop angles. *(Right)* Filtered data, keeping data only where both the strike and stop values fulfill the two inequalities in this section (V_{peak} = 169.7V). It is noted that most abnormally low and early values are eliminated though setting only an upper bound on allowable voltage.

Table 11 through Table 14 show the correlation of strike/stop phase/voltage to the key test parameters. In the case that the R_{sq}(adj) value was greater than 10%, a further analysis was conducted to determine the relationship and whether the elevated *R* value requires further consideration. *P* values in nearly all cases are equal to zero, suggesting that sufficient data were available to quantify the *R* value accurately.

Table 11. Goodness-of-fit (*R* squared values from ANOVA) for identified independent variables influencing the value of strike angle during arcing events. *N* is number of data points used in each calculation of the *R* values. *P*-values are also given for each variable.

Variable	R-Sq (%)	R-Sq (adj) (%)	P	N
Cycle Number	19.88	12.70	0.000	22728
Short-Circuit Current (I_{max})	0.77	0.75	0.000	22728
Breaker Magnetic Trip Level	0.74	0.69	0.000	22728
Iteration Number	0.43	0.42	0.000	22728
Breaker Number	0.36	0.33	0.000	22728
Manufacturer	0.18	0.17	0.000	22728
Breaker Age	0.01	0.00	0.199	22728

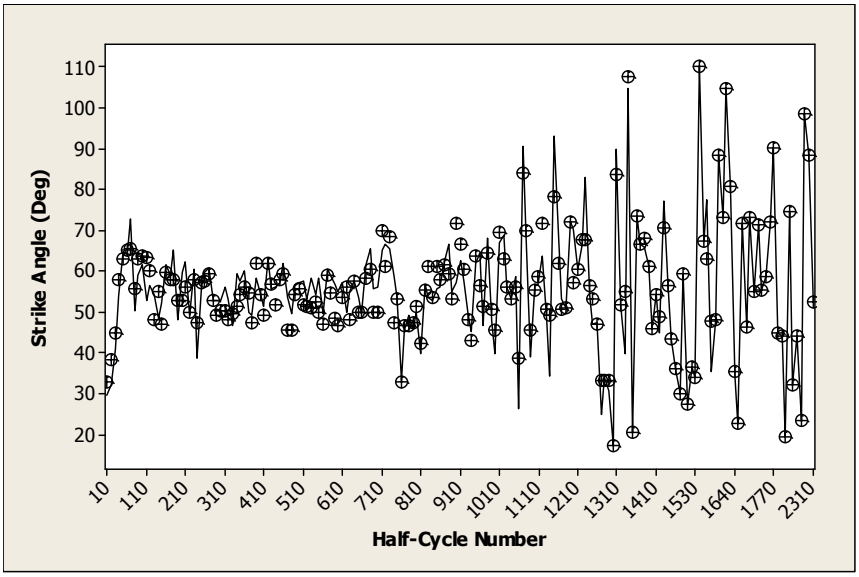

Figure 29. Mean (crosshairs) and median (solid line) values of strike angle as a function of time. Despite an R_{sq}(adj) value of 12.86%, strike angle does not show a strong correlation with time, outside lower strike angle at the start of the arcing event (half-cycle < 50).

Table 12. Goodness-of-fit (*R* squared values from ANOVA) for identified independent variables influencing the value of stop angle during arcing events. *N* is number of data points used in each calculation of the *R* values. *P*-values are also given for each variable.

Variable	R-Sq (%)	R-Sq (adj) (%)	P	N
Cycle Number	36.78	31.11	0.000	22728
Breaker Magnetic Trip Level	9.88	9.83	0.000	22728
Short-Circuit Current (I_{max})	8.78	8.77	0.000	22728
Manufacturer	4.88	4.86	0.000	22728
Breaker Age	2.83	2.82	0.000	22728
Iteration Number	1.95	1.93	0.000	22728
Breaker Number	1.88	1.85	0.000	22728

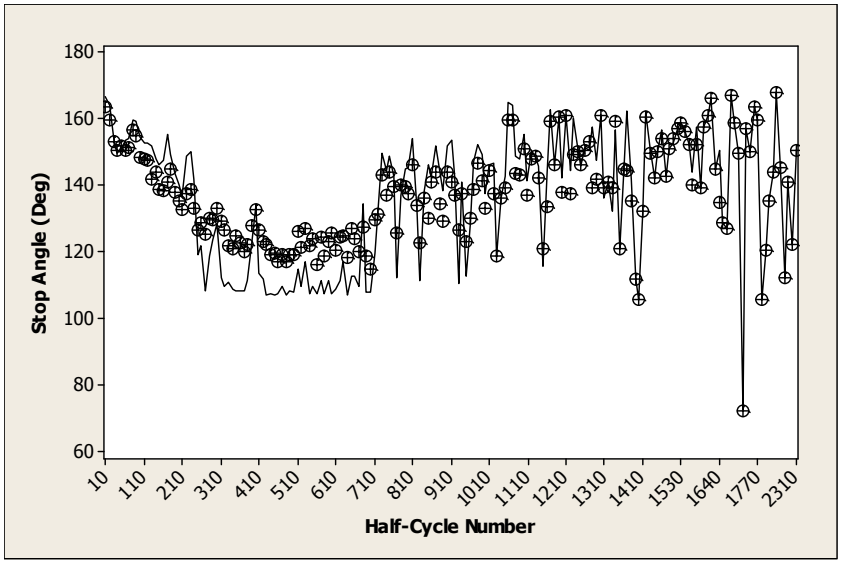

Figure 30. Mean (crosshairs) and median (solid line) values of stop angle as a function of time. The stop angle appears to decrease with time and settles on a stop angle of 110 to 120 degrees. Noisy data above 700 half-cycles is indicative of the reduced number of arcing data points.

Table 13. Goodness-of-fit (*R* squared values from ANOVA) for identified independent variables influencing the value of strike voltage during arcing events. *N* is number of data points used in each calculation of the *R* values. *P*-values are also given for each variable.

Variable	R-Sq (%)	R-Sq (adj) (%)	P	N
Short-Circuit Current (I_{max})	13.58	13.57	0.000	22728
Cycle Number	20.64	13.53	0.000	22728
Breaker Magnetic Trip Level	4.04	3.99	0.000	22728
Breaker Age	1.83	1.82	0.000	22728
Iteration Number	1.58	1.56	0.000	22728
Manufacturer	1.51	1.50	0.000	22728
Breaker Number	1.26	1.23	0.000	22728

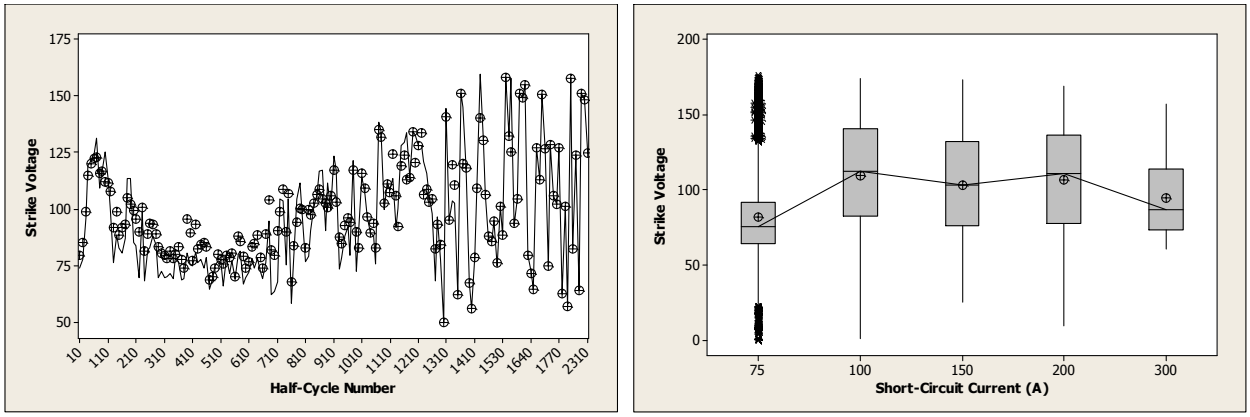

Figure 31. *(Left)* Mean (crosshairs) and median (solid line) values of strike voltage as a function of time. Strike voltage tends to be higher at the start of the arcing event, leveling off to approximately 75V. Noisy data above 700 half-cycles is indicative of the reduced number of arcing data points. *(Right)* Boxplot of strike voltage as a function of the short-circuit current. The boxplot suggests no strong correlation.

Table 14. Goodness-of-fit (*R* squared values from ANOVA) for identified independent variables influencing the value of stop voltage during arcing events. *N* is number of data points used in each calculation of the *R* values. *P*-values are also given for each variable.

Variable	R-Sq (%)	R-Sq (adj) (%)	P	N
Cycle Number	27.31	20.80	0.000	22728
Short-Circuit Current (I_{max})	3.04	3.03	0.000	22728
Breaker Magnetic Trip Level	1.39	1.34	0.000	22728
Breaker Number	0.57	0.54	0.000	22728
Manufacturer	0.52	0.51	0.000	22728
Iteration Number	0.41	0.39	0.000	22728
Breaker Age	0.01	0.01	0.135	22728

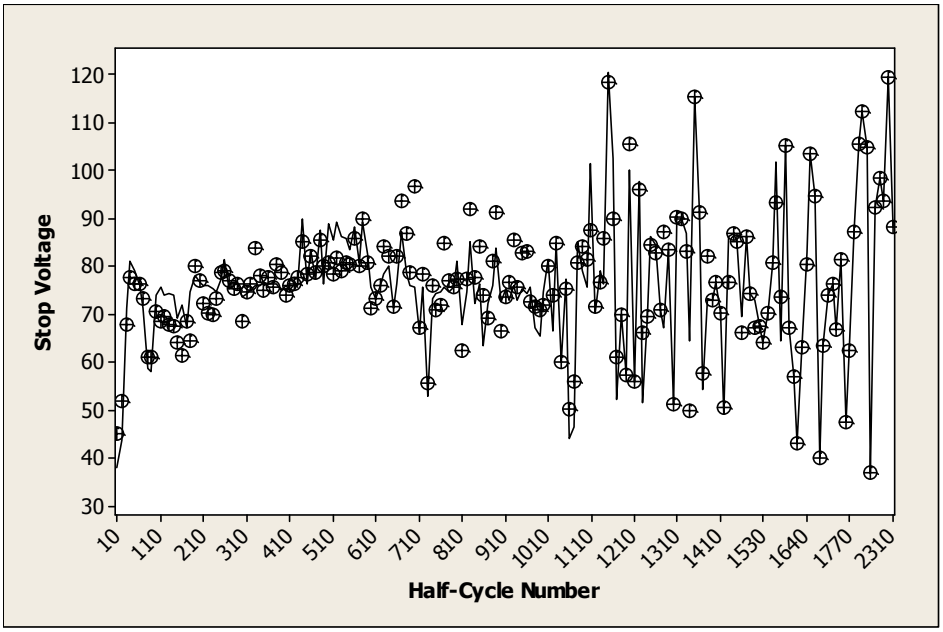

Figure 32. Mean (crosshairs) and median (solid line) values of stop voltage as a function of time. Stop voltage tends to be lower at the start of the arcing event, leveling off to approximately 80V. Noisy data above 700 half-cycles is indicative of the reduced number of arcing data points.

Conclusion of Arcing Analysis

The adjusted R_{sq} values are summarized in Table 15. The analysis shows that arcing behavior is only affected to some degree by changes in impedance of the circuit, with the most significant effect from changes in wire impedance due to heating during the test. This change is embodied in the elevated *R* values for cycle number, and reflected as well in I_{max}. A further investigation of this change shows that much of the changes occur within the first 100 half-cycles of the arcing event, reaching steady-state behavior as the event continues. This behavior was also observed in the prior UL study.[19] No other test variable, and more importantly no breaker-related test variable, had significant influence on the arcing behavior, and therefore arcing events can be treated as independent of these variables. Therefore, effects of manufacturer, breaker age, breaker position on breaker performance can be analyzed independently of arcing key parameters. In this regard, it is justifiable to consider arcing only with respect to the number and timeframe of arcing cycles, and will not require consideration of peak current, strike, and stop data when analyzing breaker performance.

Table 15. Summary of R_{sq}(adj) values for all tests (expressed by percentage), all variables in this work.

	Stop Angle	Strike Voltage	Normalized Peak Current	Stop Voltage	Strike Angle
Cycle Number	**31.11**	**13.53**	**11.85**	**20.80**	**12.70**
Short-Circuit Current (I_{max})	**8.77**	**13.57**	**18.54**	**3.03**	**0.75**
Breaker Magnetic Trip Level	**9.83**	**3.99**		**1.34**	**0.69**
Breaker Number	**1.85**	**1.23**	**1.04**	**0.54**	**0.33**
Iteration Number	**1.93**	**1.56**	**4.09**	**0.39**	**0.42**
Manufacturer	**4.86**	**1.50**	**0.90**	**0.51**	**0.17**
Breaker Age	**2.82**	**1.82**	**0.04**	**0.01**	**0.00**

≥ 40.0	30.0 – 39.9	25.0 – 29.9	20.0 – 24.9	15.0 – 19.9	10.0 – 14.9	5.00 – 9.99	1.00 – 4.99	< 1.00

Applicability of Results to Point Contact Arcing

The testing used in this work focused on carbonized path arcing, using methods as described in UL 1699, Section 40.4.[14] This was shown in an earlier work[19] to be statistically identical to the carbonized arc tests described in UL 1699, Sections 40.2 and 40.3. However, that work showed a statistical difference in strike voltage for point contact arcing tests (as described in UL 1699, Section 40.5). This difference was characterized in a change in the probability distribution function describing the strike voltage, which exhibited a lognormal distribution based on 180 degrees minus the strike voltage for Sections 40.2, 40.3, and 40.4, while for Section 40.5 the lognormal distribution was based on the untransformed strike voltage (Figure 33).[21] Table 16 shows an excerpt of the statistical distributions from that study, showing that the strike voltage for the point contact arc is expected to be lower than that from the carbonized arc. No other significant difference was identified in that study, with the resulting *R* values less than 5% for all other test variables.

[21] P.W. Brazis et al., "Synthetic Arc Generator for UL1699, Phase 2: Statistical Characterization of Arc Fault Behavior," *UL Internal Report*, 2009, page 44.

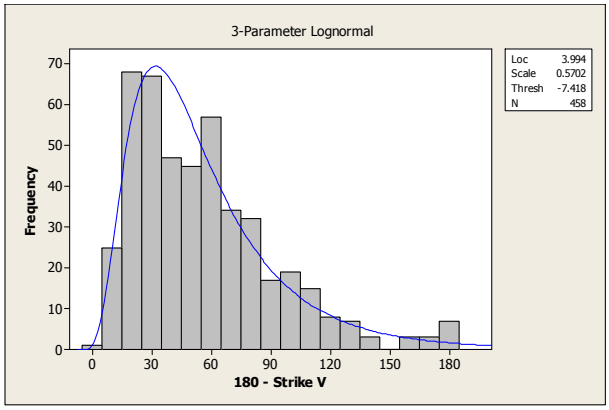

Figure 33. Example lognormal distribution fits to strike voltage data. (*Left*) Section 40.2 (carbonized path arcing), all data. (*Right*) Section 40.5 (point contact arcing), all data. Note change in *y*-axis definition, showing fit to a lognormal distribution using the untransformed strike voltage data (all data shown are filtered). From Figure 21, Ref. 21.

Table 16. Mean and standard deviations for strike voltage data by UL 1699 Section and I_{max}, derived from a normalized distribution *xform*. As can be seen, the expected strike voltage for the point contact arc is significantly less than that for the carbonized path arc. From Table 22, Ref. 21.

UL 1699 Section	I_{max}	V_{strike}, mean	V_{strike}, −1σ	V_{strike}, +1σ	V_{strike}, –95% CI	V_{strike}, +95% CI
Sec 40.2	5	143.166	107.843	162.809	47.6438	173.408
	10	134.908	102.473	154.958	52.6223	166.963
	15	116.707	72.571	143.881	4.4704	160.088
	20	100.053	41.609	135.071	−50.9968	155.404
	30	105.649	57.967	135.767	−13.7869	154.187
	45	89.150	29.196	126.386	−62.5288	148.783
	435	108.272	46.581	142.940	−57.4815	161.840
Sec 40.3	50	83.5699	51.5081	114.712	19.8383	143.768
	75	90.7128	63.2951	117.451	36.3187	142.496
	100	92.1142	57.4172	125.729	23.0572	157.011
Sec 40.4	5	135.474	98.880	160.985	48.8702	178.173
	10	135.356	102.028	159.245	57.7026	175.787
	15	135.769	110.596	155.133	79.3544	169.506
	20	129.755	100.762	151.680	64.1723	167.683
	30	126.365	100.643	146.529	69.3052	161.776
	45	113.609	85.477	135.844	51.4767	152.793
	60	107.093	81.265	128.103	50.9126	144.575
Sec 40.5	50	63.4534	36.3806	95.255	14.1862	131.000
	75	59.4741	37.7192	84.257	19.3391	111.287
	100	59.4920	35.5460	87.158	15.5926	117.752
	150	63.8726	27.6182	109.116	−0.3903	163.071
	200	66.6674	35.0381	104.808	9.7663	148.791
	300	71.3005	41.1484	107.144	16.7164	147.903

Appendix B: Statistical Analysis of Circuit Breaker Performance

The following data were the results of the ANOVA analysis of circuit breaker performance to determine the influence of key variables on different test parameters.

Table 17. Goodness-of-fit (*R* squared values from ANOVA) for identified independent variables influencing the normalized current during each test. *N* is number of data points used in each calculation of the *R* values. *P*-values are also given for each variable.

Variable	R-Sq (%)	R-Sq (adj) (%)	P	N
Short-Circuit Current (I_{max})	77.89	77.74	0.000	595
Breaker Trip	26.18	26.05	0.000	595
Breaker Magnetic Trip Level	20.68	18.91	0.000	595
Iteration Number	16.26	15.69	0.000	595
Manufacturer	9.71	9.26	0.000	595
Breaker Age	2.97	2.80	0.000	595
Breaker Number	2.02	0.85	0.100	595

Table 18. Goodness-of-fit (*R* squared values from ANOVA) for identified independent variables influencing the number of arc half-cycles during each test. *N* is number of data points used in each calculation of the *R* values. *P*-values are also given for each variable.

Variable	R-Sq (%)	R-Sq (adj) (%)	P	N
Short-Circuit Current (I_{max})	35.47	35.03	0.000	595
Iteration Number	6.11	5.47	0.000	595
Manufacturer	0.70	0.20	0.242	595
Breaker Magnetic Trip Level	1.61	0.00	0.731	595
Breaker Number	0.51	0.00	0.886	595
Breaker Age	0.16	0.00	0.329	595
Breaker Trip	0.08	0.00	0.500	595

Table 19. Goodness-of-fit (*R* squared values from ANOVA) for identified independent variables influencing the number of shorting half-cycles during each test. *N* is number of data points used in each calculation of the *R* values. *P*-values are also given for each variable.

Variable	R-Sq (%)	R-Sq (adj) (%)	P	N
Short-Circuit Current (I_{max})	45.78	45.41	0.000	595
Breaker Trip	7.21	7.06	0.000	595
Iteration Number	5.65	5.01	0.000	595
Manufacturer	0.92	0.41	0.142	595
Breaker Magnetic Trip Level	2.22	0.03	0.437	595
Breaker Number	0.59	0.00	0.838	595
Breaker Age	0.07	0.00	0.520	595

Table 20. Goodness-of-fit (*R* squared values from ANOVA) for identified independent variables influencing the time of the last arcing half-cycle during each test. *N* is number of data points used in each calculation of the *R* values. *P*-values are also given for each variable.

Variable	R-Sq (%)	R-Sq (adj) (%)	P	N
Short-Circuit Current (I_{max})	21.58	21.04	0.000	595
Breaker Trip	2.70	2.54	0.000	595
Iteration Number	2.31	1.65	0.008	595
Breaker Magnetic Trip Level	1.02	0.00	0.945	595
Breaker Number	0.53	0.00	0.872	595
Manufacturer	0.28	0.00	0.643	595
Breaker Age	0.00	0.00	0.944	595

Table 21. Goodness-of-fit (*R* squared values from ANOVA) for identified independent variables influencing the time of the last shorting half-cycle during each test. *N* is number of data points used in each calculation of the *R* values. *P*-values are also given for each variable.

Variable	R-Sq (%)	R-Sq (adj) (%)	P	N
Short-Circuit Current (I_{max})	29.63	29.15	0.000	595
Iteration Number	4.57	3.92	0.000	595
Breaker Magnetic Trip Level	1.09	0.00	0.930	595
Breaker Number	0.67	0.00	0.784	595
Manufacturer	0.06	0.00	0.949	595
Breaker Trip	0.05	0.00	0.584	595
Breaker Age	0.00	0.00	0.984	595

Table 22. Goodness-of-fit (*R* squared values from ANOVA) for identified independent variables influencing the time of circuit breaker trip during each test. *N* is number of data points used in each calculation of the *R* values. *P*-values are also given for each variable.

Variable	R-Sq (%)	R-Sq (adj) (%)	P	N
Breaker Trip	95.05	95.04	0.000	595
Short-Circuit Current (I_{max})	40.14	39.73	0.000	595
Breaker Magnetic Trip Level	17.19	15.34	0.000	595
Manufacturer	11.85	11.41	0.000	595
Iteration Number	8.92	8.30	0.000	595
Breaker Age	0.57	0.40	0.066	595
Breaker Number	0.79	0.00	0.702	595

Table 23. Summary of R_{sq}(adj) values for all tests (expressed by percentage), all variables in this work.

	Normalized Current	Time of Circuit Breaker Trip	Number of Shorting Half-Cycles	Number of Arcing Half-Cycles	Last Shorting Half-Cycle	Last Arcing Half-Cycle
Short-Circuit Current (I_{max})	**77.74**[†]	**39.73**	**45.41**	**35.03**	**29.15**	**21.04**
Iteration Number	**15.69**[††]	**8.30**	**5.01**	**5.47**	**3.92**	**1.65**
Breaker Trip	**26.05**	**95.04**[‡‡]	**7.06**	**0.00**	**0.00**	**2.54**
Breaker Magnetic Trip Level	**18.91**[†]	**15.34***	**0.03**	**0.00**	**0.00**	**0.00**
Manufacturer	**9.26**[‡]	**11.41***,[‡]	**0.41**	**0.20**	**0.00**	**0.00**
Breaker Age	**2.80**	**0.40**	**0.00**	**0.00**	**0.00**	**0.00**
Breaker Number	**0.85**	**0.00**	**0.00**	**0.00**	**0.00**	**0.00**

[*] Correlation due to range of testing: breakers with lower magnetic trip level trip more often in project than those with higher trip level. More meaningful to use normalized current for analysis.

[†] High correlation since normalized current is defined in terms of magnetic trip level and I_{max}.

[††] Correlation due to more iterations conducted at higher currents, fewer at lower currents. Correlation is negligible if broken down by I_{max}, see Figure 34. This correlation reflects into all other variables, showing artificially elevated R values and therefore can be neglected.

[‡] Manufacturer D breakers had consistently lower magnetic trip levels than other manufacturers, this influenced normalized current and breaker trip data. Using the normalized current remedies this issue.

[‡‡] High correlation since breaker trip is calculated directly from the time of circuit breaker trip.

≥ 40.0	30.0 – 39.9	25.0 – 29.9	20.0 – 24.9	15.0 – 19.9	10.0 – 14.9	5.00 – 9.99	1.00 – 4.99	< 1.00

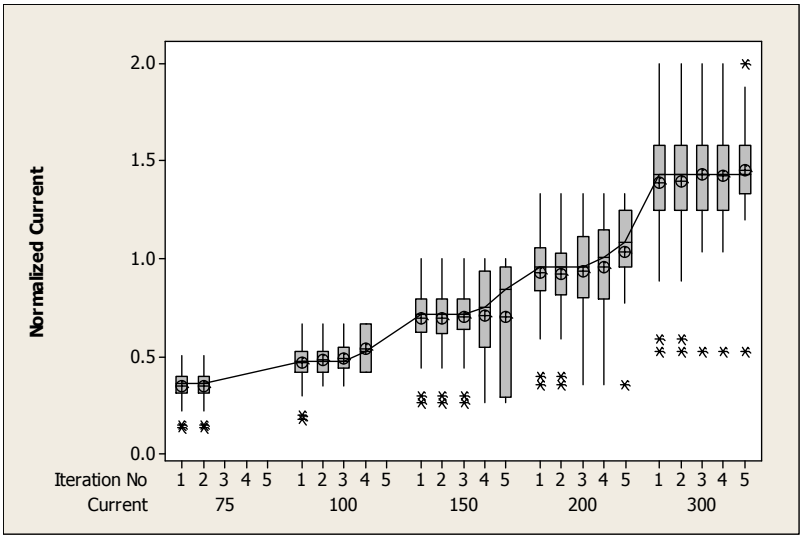

Figure 34. Boxplot of normalized current as a function of iteration number and short-circuit current (I_{max}). This figure shows that the *R* value correlating iteration number to normalized current is an artifact of nonuniform testing (more iterations at higher current), and that the iteration itself does not influence the data.